

# Charged Lepton Flavor Violation Experiments\*

William J. Marciano,<sup>1</sup> Toshinori Mori,<sup>2</sup>  
and J. Michael Roney<sup>3</sup>

<sup>1</sup>Brookhaven National Laboratory, Upton, New York 11973; email: marciano@bnl.gov

<sup>2</sup>International Center for Elementary Particle Physics, The University of Tokyo, Tokyo 113-0033, Japan; email: mori@icepp.s.u-tokyo.ac.jp

<sup>3</sup>Department of Physics and Astronomy, University of Victoria, Victoria, British Columbia V8W 3P6, Canada; email: mronney@uvic.ca

Annu. Rev. Nucl. Part. Sci. 2008. 58:315–41

First published online as a Review in Advance on July 29, 2008

The *Annual Review of Nuclear and Particle Science* is online at [nucl.annualreviews.org](http://nucl.annualreviews.org)

This article's doi:  
10.1146/annurev.nucl.58.110707.171126

Copyright © 2008 by Annual Reviews.  
All rights reserved

0163-8998/08/1123-0315\$20.00

\*The U.S. Government has the right to retain a nonexclusive, royalty-free license in and to any copyright covering this paper.

## Key Words

electron, muon, tau

## Abstract

We provide a review of the status of experimental searches for lepton flavor violation involving electrons, muons, and tau leptons. Future experimental programs are discussed and placed in the context of theories beyond the standard model.

## Contents

1. INTRODUCTION .....	316
1.1. Flavor Changing Neutral Currents .....	317
1.2. Electromagnetic Transitions .....	319
1.3. Neutrino Masses and Mixing .....	320
1.4. The Muon Anomalous Magnetic Moment and Lepton Flavor Violations .....	321
2. RARE MUON DECAYS AND REACTIONS .....	323
2.1. $\mu^+ \rightarrow e^+ \gamma$ .....	323
2.2. $\mu^\pm \rightarrow e^\pm e^+ e^-$ .....	326
2.3. $\mu - e$ Conversion .....	326
3. LEPTON FLAVOR VIOLATION IN TAU LEPTON DECAYS .....	329
3.1. Tau Lepton Data Samples and Search Strategies .....	329
3.2. Current Results on Lepton Flavor Violation Decays of the Tau .....	333
3.3. Future Prospects .....	335
4. SEARCHES FOR CHARGED LEPTON FLAVOR VIOLATION IN MESON DECAYS .....	336
5. SEARCHES FOR CHARGED LEPTON FLAVOR VIOLATION IN $Z^0$ DECAYS .....	337
6. SUMMARY AND OUTLOOK .....	339

## 1. INTRODUCTION

After more than a century of great discoveries, we now have a standard model of elementary particle physics. It describes three generations of fundamental spin  $\frac{1}{2}$  fermions (quarks and leptons), each containing particles of electric charges  $\frac{2}{3}$ ,  $-\frac{1}{3}$ , 0, and  $-1$  (and their antiparticles). Grouped by (ordered) mass eigenstates, they are:

First generation	u,	d,	$\nu_1$ ,	e
Second generation	c,	s,	$\nu_2$ ,	$\mu$
Third generation	t,	b,	$\nu_3$ ,	$\tau$ .

Neutrino masses (the newest addition to the standard model paradigm),  $m_1$ ,  $m_2$ , and  $m_3$ , are very small [ $< \mathcal{O}(1 \text{ eV})$ ], whereas the top quark is extremely heavy ( $\sim 171 \text{ GeV}$ ). Other quarks and charged leptons have masses in between these extremes, showing no discernible pattern (1). Is the top quark anomalously massive or are the other fermions unusually light? Deciphering the spectrum of fermion masses is an outstanding problem in elementary particle physics.

Interactions among elementary particles are described by  $SU(3)_C \times SU(2)_L \times U(1)_Y$  local gauge symmetries whereby strong, weak, and electromagnetic forces are mediated by gluons,  $W^\pm$ ,  $Z^0$ , and  $\gamma$  spin 1 bosons. Standard model weak interaction properties and predictions have been successfully tested at approximately the  $\pm 0.1\%$  level by probing tree level as well as quantum loop effects. (The standard model's quantum electrodynamics sector, of course, has been much more precisely established.) Only the anticipated spin-0 Higgs scalar particle, a remnant of  $SU(2)_L \times U(1)_Y$  electroweak symmetry breaking and mass generation, remains undiscovered with a current experimental lower bound on  $m_{\text{Higgs}}$  from direct searches of 114.4 GeV (2) and a quantum loop indirect upper bound of 144 GeV (3). Nevertheless, it is anticipated that some new physics beyond standard model expectations, such as supersymmetric particle partners, heavy fermions, additional gauge bosons, strong dynamics, etc., will eventually emerge that will help explain some of the

observed subtle features of nature, including the true origin of the broadly disparate masses, parity violation, and three distinct generations.

The primary way to uncover new physics is to explore the high-energy frontier at colliders, where heavy new particles can be directly produced and studied. Less direct means, which are complementary and in some cases capable of exploring much higher mass scales (even  $> 1000$  TeV), involve searches for new physics in rare or highly suppressed flavor changing neutral current reactions. Experimental searches for such effects involving charged leptons ( $e$ ,  $\mu$ , and  $\tau$ ) are the subject of this review.

### 1.1. Flavor Changing Neutral Currents

Individual quarks and leptons are assigned a quantum number called flavor. For example, electron, muon, and tau numbers (or flavors) are assigned to the charged leptons. Flavor is conserved at the tree level by all neutral current interactions (mediated by gluons,  $Z^0$ , and  $\gamma$ ), but is violated in charged current weak interactions mediated by  $W^\pm$  bosons. Due to mixing among generations of fermions, charged current loop effects can induce flavor changing weak neutral current interactions at the quantum level. Naïvely, such effects could be of  $\mathcal{O}(\alpha/\pi) \simeq \frac{1}{400}$  relative to ordinary weak interactions, but in fact they are often found to be much more strongly suppressed.

In the case of quarks, such loop-induced effects lead to small but observable  $s \rightarrow d$  transitions. Their observed suppression, e.g., in  $K_L^0 \rightarrow \mu^+ \mu^-$ , was extremely important in unveiling the existence of charm via the GIM (Glashow–Iliopolous–Maiani) mechanism (4) and in predicting its properties. Such loops were also instrumental in explaining CP violation as a manifestation of predicted three-generation Cabibbo–Kobayashi–Maskawa (CKM) mixing. More recently, the study of CP violation in  $b \rightarrow d$  amplitudes confirmed the CKM model (5, 6). Also, the measurement of  $b \rightarrow s \gamma$  decays and the search for  $B_s \rightarrow \mu^+ \mu^-$  have been at the forefront of (low-energy) supersymmetry (SUSY) constraints.

In the case of charged leptons, searches for flavor changing neutral current effects have, so far, yielded null results. Nevertheless, they have had important historical significance. For example, the nonobservation of  $\mu \rightarrow e \gamma$  during the early days following the discovery of the muon (7) helped establish the muon as a distinct elementary lepton rather than an excited electron (8). The same is true for the early tau days, when lack of  $\tau^\pm \rightarrow e^\pm \gamma$  and  $\tau^\pm \rightarrow \mu^\pm \gamma$  decays helped establish the tau as elementary. Follow-up constraints on  $\mathcal{B}(\mu^+ \rightarrow e^+ \gamma)$  below  $\sim 10^{-5}$  were later used to argue for the existence of a second neutrino (the  $\nu_\mu$ ) needed to cancel possible large but unobserved loop-induced neutral current effects inferred in a single-neutrino scenario (9). The search and subsequent discovery of the second neutrino (10) using neutrino beams (11, 12) was not only a quantum loop success, but it also led to the establishment of accelerator-based neutrino physics as a viable science. Introduction of the  $\nu_\mu$  to suppress flavor changing neutral current charged lepton interactions was completely analogous to the GIM mechanism introduction of charm to suppress strangeness changing neutral currents (13, 14).

The sensitivity in the search for  $\mu^+ \rightarrow e^+ \gamma$  and other rare lepton flavor violating (LFV) reactions has been increased by many orders of magnitude over the years (shown in **Figure 1**). As the bounds were lowered, speculative theoretical new physics models were ruled out or constrained. Some current experimental bounds on various LFV reactions are given in **Table 1**, where we also list goals of ongoing, proposed, and possible future experiments. Most of the bounds are from unobserved decays such as  $\mu^+ \rightarrow e^+ \gamma$ ,  $\mu^\pm \rightarrow e^\pm e^+ e^-$ ,  $\tau^\pm \rightarrow \mu^\pm \gamma$ ,  $\tau^\pm \rightarrow \mu^\pm \mu^+ \mu^-$ , etc. However, one very stringent constraint (currently the best bound) comes from the search for coherent  $\mu^- \rightarrow e^-$  conversions in the field of a nucleus,  $\mu^- N \rightarrow e^- N$ . It potentially occurs in the following sequential manner. Stopped muons are quickly captured by atoms ( $\sim 10^{-10}$  s) and

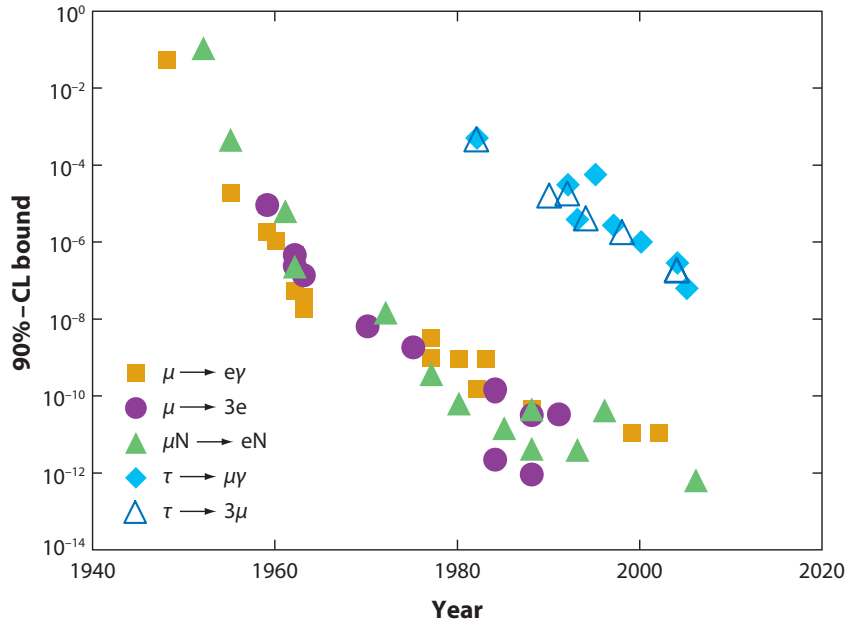


**Figure 1**

Record of selected lepton flavor violation searches.

cascade down to 1S orbitals. There, they can undergo (a) ordinary decay with a rate of  $\sim 5 \times 10^5 \text{ s}^{-1}$ , (b) weak capture,  $\mu^- \text{p} \rightarrow \nu_\mu \text{n}$  (which exceeds the ordinary decay rate for nuclei with  $Z > 6$ ), or (c) coherent flavor changing conversion,  $\mu^- N \rightarrow e^- N$ . The last of these reactions has already been significantly constrained using various targets. Indeed, the ratio of conversions to capture,

**Table 1** A sample of various charged lepton flavor violating reactions

Reaction	Current bound	Reference	Expected	Possible
$\mathcal{B}(\mu^+ \rightarrow e^+ \gamma)$	$< 1.2 \times 10^{-11}$	28	$2 \times 10^{-13}$	$2 \times 10^{-14}$
$\mathcal{B}(\mu^\pm \rightarrow e^\pm e^+ e^-)$	$< 1.0 \times 10^{-12}$	37	–	$10^{-14}$
$\mathcal{B}(\mu^\pm \rightarrow e^\pm \gamma \gamma)$	$< 7.2 \times 10^{-11}$	92	–	–
$R(\mu^- \text{Au} \rightarrow e^- \text{Au})$	$< 7 \times 10^{-13}$	15	–	–
$R(\mu^- \text{Al} \rightarrow e^- \text{Al})$	–		$10^{-16}$	$10^{-18}$
$\mathcal{B}(\tau^\pm \rightarrow \mu^\pm \gamma)$	$< 5.9 \times 10^{-8}$	<b>Table 2</b>		$\mathcal{O}(10^{-9})$
$\mathcal{B}(\tau^\pm \rightarrow e^\pm \gamma)$	$< 8.5 \times 10^{-8}$	<b>Table 2</b>		$\mathcal{O}(10^{-9})$
$\mathcal{B}(\tau^\pm \rightarrow \mu^\pm \mu^+ \mu^-)$	$< 2.0 \times 10^{-8}$	<b>Table 2</b>		$\mathcal{O}(10^{-10})$
$\mathcal{B}(\tau^\pm \rightarrow e^\pm e^+ e^-)$	$< 2.6 \times 10^{-8}$	<b>Table 2</b>		$\mathcal{O}(10^{-10})$
$Z^0 \rightarrow e^\pm \mu^\mp$	$< 1.7 \times 10^{-6}$	90		
$Z^0 \rightarrow e^\pm \tau^\mp$	$< 9.8 \times 10^{-6}$	90		
$Z^0 \rightarrow \mu^\pm \tau^\mp$	$< 1.2 \times 10^{-5}$	91		
$K_L^0 \rightarrow e^\pm \mu^\mp$	$< 4.7 \times 10^{-12}$	74		$10^{-13}$
$D^0 \rightarrow e^\pm \mu^\mp$	$< 8.1 \times 10^{-7}$	78		$10^{-8}$
$B^0 \rightarrow e^\pm \mu^\mp$	$< 9.2 \times 10^{-8}$	79		$10^{-9}$

Data from current experimental bounds, expected improvements from existing or funded experiments, and possible long-term advances.

$$R(\mu^- N \rightarrow e^- N) = \frac{\omega(\mu^- N \rightarrow e^- N)}{\omega(\mu^- N \rightarrow \nu_\mu N)}, \quad 1.$$

has reached the  $<7 \times 10^{-13}$  bound for gold nuclei (15), and a similar (unpublished) result by the same SINDRUM II collaboration exists for titanium. The simplicity and distinctive signal, a monoenergetic electron of energy

$$E_{\text{mec}} = m_\mu - B_\mu(Z, A) - R(A) \sim 105 \text{ MeV}, \quad 2.$$

where  $m_\mu$  is the muon mass,  $B_\mu(Z, A)$  is the muonic atom binding energy, and  $R(A)$  is the nuclear recoil energy for a nucleus with atomic number  $Z$  and mass number  $A$ , promise to allow the bound or discovery potential to be pushed much further. Indeed, with only a single final-state particle (as opposed to two in  $\mu^+ \rightarrow e^+ \gamma$ ), accidentals are not a problem and extremely high rates are possible. Those features allow the unique opportunity of pushing  $R(\mu^- N \rightarrow e^- N)$  to  $10^{-17} \sim 10^{-18}$ . This represents an improvement in sensitivity of four to five orders of magnitude over current bounds, which in a mature experimental area is generally unheard of.

## 1.2. Electromagnetic Transitions

Radiative decays of the generic form  $\ell_1 \rightarrow \ell_2 + \gamma$  ( $\ell_1 = \mu, \tau$ ;  $\ell_2 = e, \mu$ ) proceed through electromagnetic gauge-invariant transition amplitudes of the form

$$\mathcal{M} = \frac{e G_F m_{\ell_1}}{16\sqrt{2}\pi^2} \varepsilon^\mu q^\nu \bar{\ell}_2(p_2) \sigma_{\mu\nu} \left( D_R \frac{1 + \gamma_5}{2} + D_L \frac{1 - \gamma_5}{2} \right) \ell_1(p_1), \quad 3.$$

where  $q = p_1 - p_2$  and  $\sigma_{\mu\nu} = \frac{i}{2}[\gamma_\mu, \gamma_\nu]$ ; we have normalized with respect to the Fermi constant,  $G_F = 1.16637(1) \times 10^{-5} \text{ GeV}^{-2}$ , along with a  $\frac{1}{16}\pi^2$  that generally results from a loop integration.  $D_R$  and  $D_L$  are model-dependent transition dipole moments. For  $m_{\ell_2} \ll m_{\ell_1}$ , that amplitude leads to the decay rate

$$\Gamma(\ell_1 \rightarrow \ell_2 \gamma) = \frac{\alpha G_F^2 m_{\ell_1}^5}{2048\pi^4} (|D_R|^2 + |D_L|^2) \quad 4.$$

and the branching ratio

$$\mathcal{B}(\ell_1 \rightarrow \ell_2 \gamma) = \frac{3\alpha}{32\pi} (|D_R|^2 + |D_L|^2) \mathcal{B}(\ell_1 \rightarrow \ell_2 \nu \bar{\nu}), \quad 5.$$

where  $\mathcal{B}(\mu \rightarrow e \nu \bar{\nu}) \simeq 1$  and  $\mathcal{B}(\tau \rightarrow \mu \nu \bar{\nu}) = 0.973 \mathcal{B}(\tau \rightarrow e \nu \bar{\nu}) \simeq 0.1736$ . The amplitude of Equation 3 results from a dimension-five operator that cannot exist at tree level in a renormalizable theory. It can and generally will be induced at loop level due to LFV effects (16, 17).

To obtain a rough estimate regarding the mass scale of new physics probed by searches such as  $\mu^+ \rightarrow e^+ \gamma$ , we can reparameterize the amplitude in Equation 3 by  $e m_\mu / \Lambda^2 \varepsilon^\mu q^\nu \bar{e} \sigma_{\mu\nu} \mu$  or  $D_R = D_L = 16\sqrt{2}\pi^2 / G_F \Lambda^2$ , where  $\Lambda$  is the scale of new physics responsible for muon number violation. Comparing this result with the current bound on  $\mathcal{B}(\mu^+ \rightarrow e^+ \gamma)$  in **Table 1** leads to the constraint  $\Lambda \geq 340 \text{ TeV}$ . Of course, the bound depends on exactly how we parameterize the new physics. Nevertheless, such a stringent constraint, which will be extended to about  $\sim 1000 \text{ TeV}$  by an ongoing Paul Scherrer Institut (PSI) effort, nicely illustrates the reach of LFV reactions. For a detailed discussion on how rare muon decays probe new physics, we refer the reader to the thorough 1999 review by Kuno & Okada (18).

The photon amplitude above can also give rise to  $\ell_1 \rightarrow \ell_2 \bar{\ell}_2 \ell_2$  via a virtual photon. One finds (for  $m_{\ell_2} \ll m_{\ell_1}$ ) (18)

$$\frac{\mathcal{B}(\ell_1 \rightarrow 3\ell_2)}{\mathcal{B}(\ell_1 \rightarrow \ell_2 \gamma)} \simeq \frac{\alpha}{3\pi} \left[ \ln \left( \frac{m_{\ell_1}^2}{m_{\ell_2}^2} \right) - \frac{11}{4} \right], \quad 6.$$

which gives  $\mathcal{B}(\mu \rightarrow 3e)/\mathcal{B}(\mu \rightarrow e\gamma) \simeq 0.006$ . Of course, additional amplitudes (not of the chiral changing structure in Equation 3) such as  $\mathcal{M} = i\frac{4G_F}{\sqrt{2}}g\bar{e}_L\gamma_\mu\mu_L\bar{e}_L\gamma^\mu e_L$ , which gives rise to  $\mathcal{B}(\mu \rightarrow 3e) \approx 2g^2$ , could substantially increase  $\mathcal{B}(\ell_1 \rightarrow 3\ell_2)$  relative to  $\mathcal{B}(\ell_1 \rightarrow \ell_2\gamma)$  in some new physics scenarios. Indeed, one can often find  $\mathcal{B}(\ell_1 \rightarrow 3\ell_2) > \mathcal{B}(\ell_1 \rightarrow \ell_2\gamma)$ , which could be particularly important for  $\tau^\pm \rightarrow \mu^\pm\mu^+\mu^-$  decays: Experiments searching for this three-muon mode are expected to have a greater sensitivity than  $\tau^\pm \rightarrow \mu^\mp\gamma$  because of its particularly clean experimental signature of three final-state muons.

In the case of coherent muon-electron conversion in the field of a nucleus, attaching the photon from the amplitude in Equation 3 to the nuclear Coulombic field leads to the coherent rate ratio

$$R(\mu^- N \rightarrow e^- N) \simeq \frac{G_F^2 m_\mu^4}{96\pi^3 \alpha} \times 3 \times 10^{12} B(A, Z) \mathcal{B}(\mu \rightarrow e\gamma), \quad 7.$$

where  $B(A, Z)$  is a nucleus-dependent factor that includes atomic and nuclear effects. One finds  $B = 1.1, 1.8,$  and  $1.25$  for Al, Ti, and Pb, respectively (19, 20). [Pb and Au have similar  $B(A, Z)$  factors.]

For the example of  $N = \text{Al}$ , one finds,

$$\mathcal{B}(\mu \rightarrow e\gamma) \simeq 389 R(\mu^- \text{Al} \rightarrow e^- \text{Al}). \quad 8.$$

Indeed, if the amplitude in Equation 3 dominates,

$$\mathcal{B}(\mu \rightarrow e\gamma) : \mathcal{B}(\mu \rightarrow 3e) : R(\mu^- \text{Al} \rightarrow e^- \text{Al}) :: 389 : 2.3 : 1, \quad 9.$$

suggesting that  $\mu$ -e coherent conversion comes in third. Experimentally, however, conversion can be pushed three to four orders of magnitude beyond the other reactions. In addition, for many types of new physics scenarios the amplitude in Equation 3 does not dominate. Instead, relatively large chiral conserving amplitudes of the form  $\bar{e}\gamma_\mu\mu\bar{q}\gamma^\mu q$  could enhance  $R(\mu^- N \rightarrow e^- N)$  relative to  $\mathcal{B}(\mu^+ \rightarrow e^+\gamma)$ . In fact, the coherent conversion can easily be  $\mathcal{O}(100)$  times larger, as we discuss below.

### 1.3. Neutrino Masses and Mixing

We now know that lepton flavor is not exactly conserved. Flavor nonconserving mixing among generations has been observed in neutrino oscillations (1). Neutrinos produced by weak interactions ( $\nu_e, \nu_\mu,$  and  $\nu_\tau$ ) are related to the mass eigenstates ( $\nu_1, \nu_2,$  and  $\nu_3$ ) via

$$\begin{pmatrix} |\nu_e\rangle \\ |\nu_\mu\rangle \\ |\nu_\tau\rangle \end{pmatrix} = U \begin{pmatrix} |\nu_1\rangle \\ |\nu_2\rangle \\ |\nu_3\rangle \end{pmatrix} \quad 10.$$

$$U = \begin{pmatrix} c_{12}c_{13} & s_{12}c_{13} & s_{13}e^{-i\delta} \\ -s_{12}c_{23} - c_{12}s_{23}s_{13}e^{i\delta} & c_{12}c_{23} - s_{12}s_{23}s_{13}e^{i\delta} & s_{23}c_{13} \\ s_{12}s_{23} - c_{12}c_{23}s_{13}e^{i\delta} & -c_{12}s_{23} - s_{12}c_{23}s_{13}e^{i\delta} & c_{23}c_{13} \end{pmatrix}$$

$$c_{ij} = \cos\theta_{ij}, \quad s_{ij} = \sin\theta_{ij}, \quad i, j = 1, 2, 3.$$

From a combination of solar, reactor, atmospheric, and accelerator neutrino oscillation results (1), we now know that (roughly)

$$\begin{aligned}\Delta m_{32}^2 &= m_3^2 - m_2^2 \simeq \pm 2.5 \times 10^{-3} \text{ eV}^2 \\ \Delta m_{21}^2 &= m_2^2 - m_1^2 \simeq 8 \times 10^{-5} \text{ eV}^2\end{aligned}\quad 11.$$

$$\begin{aligned}\sin^2 2\theta_{23} &\simeq 1 & \sin^2 2\theta_{12} &\simeq 0.80 \\ \sin^2 2\theta_{13} &< 0.15 & 0 \leq \delta < 360^\circ.\end{aligned}\quad 12.$$

The mixing is relatively large (although  $\theta_{13}$  is currently unknown), but the mass differences are extremely small compared to the weak scale ( $m_W \simeq 80.4 \text{ GeV}$ ), resulting in accidental approximate lepton flavor conservation. Computing the  $D_R$  and  $D_L$  in Equation 3 due to neutrino loops gives for  $\ell_1 = \mu, \ell_2 = e$

$$D_L \simeq \frac{1}{2} \sin 2\theta_{13} \sin \theta_{23} e^{-i\delta} \frac{\Delta m_{32}^2}{m_W^2}, \quad D_R = 0$$

or

$$\mathcal{B}(\mu^+ \rightarrow e^+ \gamma) \simeq 10^{-54} \left( \frac{\sin^2 2\theta_{13}}{0.15} \right), \quad 13.$$

which is nonzero (if  $\sin^2 2\theta_{13} \neq 0$ ), but which is much too small to access experimentally. Therefore, the actual observation of  $\mu^+ \rightarrow e^+ \gamma$  at  $\mathcal{O}(10^{-12} - 10^{-13})$  would clearly indicate a signal for new physics beyond negligible, ordinary neutrino mass effects.

In the case of coherent  $\mu^- N \rightarrow e^- N$  conversion, the  $W^+ W^-$  loop box diagrams dominate and one finds (roughly) from chiral conserving loop amplitudes (16)

$$R(\mu^- \text{Al} \rightarrow e^- \text{Al}) \simeq 2 \times 10^{-52} \frac{\sin^2 2\theta_{13}}{0.15}. \quad 14.$$

Again, the predicted rate is negligibly small. However, the rate in Equation 14 is about 200 times larger than that in Equation 13 (16, 17) and illustrates the possibility of  $R(\mu^- N \rightarrow e^- N)$  being larger than  $\mathcal{B}(\mu^+ \rightarrow e^+ \gamma)$ . The neutrino example also illustrates what can happen if heavy neutrinos exist and mix with the light ones. For a fourth generation with neutrinos  $\mathcal{N}$  and mixing-induced couplings  $U_{e\mathcal{N}}$  and  $U_{\mu\mathcal{N}}$  with the electron and muon, respectively, one finds

$$\mathcal{B}(\mu^+ \rightarrow e^+ \gamma) \simeq \frac{3\alpha}{32\pi} |U_{e\mathcal{N}}^* U_{\mu\mathcal{N}}|^2 \frac{m_{\mathcal{N}}^4}{m_W^4}. \quad 15.$$

For  $m_{\mathcal{N}} \simeq m_W$ ,  $|U_{e\mathcal{N}}^* U_{\mu\mathcal{N}}|$  is already constrained to be less than  $\sim 2 \times 10^{-4}$ . In the case of  $R(\mu^- N \rightarrow e^- N)$ , the  $W^+ W^-$  box diagram with a heavy  $\mathcal{N}$  dominates, and one finds (roughly) for  $m_{\mathcal{N}} \simeq m_W$

$$R(\mu^- \text{Al} \rightarrow e^- \text{Al}) \simeq 4\mathcal{B}(\mu^+ \rightarrow e^+ \gamma). \quad 16.$$

In such an example, coherent  $\mu$ -e conversion can be a more powerful probe of heavy neutrino mixing than  $\mu^+ \rightarrow e^+ \gamma$ .

#### 1.4. The Muon Anomalous Magnetic Moment and Lepton Flavor Violations

The muon anomalous magnetic moment,  $a_\mu \equiv \frac{g_\mu - 2}{2}$ , is very similar in structure to Equation 3, except that it is flavor diagonal ( $\ell_1 = \ell_2 = \mu$ ); i.e., it conserves lepton flavor and has no  $\gamma_5$  term. It is quite sensitive to some types of new physics, such as SUSY, due to its chiral changing Lorentz

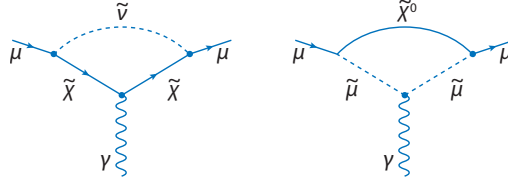


**Figure 2**

Potential supersymmetric contributions to muon  $g-2$  (21).

structure. If new physics manifests itself in  $a_\mu$ , it is likely that flavor violation in the new physics sector will also show up in  $\mu^+ \rightarrow e^+ \gamma$  and other LFV reactions (21, 22).

Currently, there is a  $3.4\text{-}\sigma$  discrepancy between experiment and the standard model prediction for  $a_\mu$  (1):

$$\begin{aligned} a_\mu^{\text{exp}} &= 116\,592\,080(63) \times 10^{-11}, \\ a_\mu^{\text{SM}} &= 116\,591\,788(58) \times 10^{-11}, \\ \Delta a_\mu &= a_\mu^{\text{exp}} - a_\mu^{\text{SM}} = 292(63)(58) \times 10^{-11}. \end{aligned} \quad 17.$$

The difference, which is sizeable, could indicate an underestimate of standard model hadronic loop effects or a more exciting new physics possibility. In the latter case, the scale of new physics is likely to be in the 100 GeV–2 TeV range, with relatively low-mass scale SUSY being the most natural candidate explanation (see **Figure 2**).

If new physics is responsible for  $\Delta a_\mu$ , it should also give rise to off-diagonal LFV electromagnetic transition amplitudes of the type shown in Equation 3, albeit at a reduced level due to the requirement of flavor violation (23, 24). (These amplitudes for SUSY-induced LFV radiative decays are similar to those shown in **Figure 2**, but with different charged leptons in the initial and final states.) Indeed, one expects (roughly)

$$D_R(\text{and/or } D_L) \simeq \frac{16\sqrt{2}\pi^2}{G_F m_\mu^2} \Delta a_\mu \varepsilon_{\ell_1 \ell_2}, \quad 18.$$

where the  $\varepsilon_{\ell_1 \ell_2}$  parameterize the (model-dependent) flavor violating suppression factors. Assuming such a relationship, one expects from Equation 5

$$\mathcal{B}(\ell_1 \rightarrow \ell_2 \gamma) \simeq 6.4 \times 10^{14} (\Delta a_\mu)^2 |\varepsilon_{\ell_1 \ell_2}|^2 \mathcal{B}(\ell_1 \rightarrow \ell_2 \nu \bar{\nu}). \quad 19.$$

For the cases of interest (using  $\Delta a_\mu$  in Equation 17),

$$\begin{aligned} \mathcal{B}(\mu^+ \rightarrow e^+ \gamma) &\simeq 6 \times 10^{-3} |\varepsilon_{e\mu}|^2 \\ \mathcal{B}(\tau^\pm \rightarrow \mu^\pm \gamma) &\simeq 1 \times 10^{-3} |\varepsilon_{\mu\tau}|^2 \\ \mathcal{B}(\tau^\pm \rightarrow e^\pm \gamma) &\simeq 1 \times 10^{-3} |\varepsilon_{e\tau}|^2. \end{aligned} \quad 20.$$

Other LFV rates may be estimated from the relationships described in Section 1.2.

Comparing with the bounds in **Table 1** we see that small  $\varepsilon_{\ell_1 \ell_2}$  suppression factors are needed, particularly for  $\varepsilon_{e\mu}$ , where the current bound on  $\mathcal{B}(\mu^+ \rightarrow e^+ \gamma)$  already requires  $\varepsilon_{e\mu} \leq 4.5 \times 10^{-5}$ . What makes such a bound particularly interesting is that some models such as SUSY suggest that  $\varepsilon_{e\mu}$  should be of order this bound. In fact,  $\varepsilon_{e\mu}$  is only small due to a super-GIM mechanism requiring near-mass degeneracies among different generations of superparticles (sparticles).

Indeed, for large mixing this bound translates into a constraint on slepton mass degeneracies within loops

$$\frac{\Delta M^2}{M^2} \simeq \frac{M_1^2 - M_2^2}{M_1^2} < 10^{-4} \quad 21.$$

or very roughly

$$M_1 - M_2 < 4.5 \times 10^{-5} M_1. \quad 22.$$

So, for sparticle masses of order several hundred gigaelectronvolts, the degeneracy between generations must be in the tens of megaelectronvolts. Stated differently, if the current  $\Delta a_\mu \neq 0$  result is caused by new physics, observation of  $\mu^+ \rightarrow e^+ \gamma$  may be right around the corner.

In the case of tau decays, one might expect a larger breaking of third-generation sparticle degeneracy (relative to the first and second generations). That being the case, and assuming reasonable mixing, rare decays such as  $\tau^\pm \rightarrow \mu^\pm \gamma$  and  $\tau^\pm \rightarrow e^\pm \gamma$  may be observable at the  $10^{-9}$  level.

## 2. RARE MUON DECAYS AND REACTIONS

The best-studied rare muon decays and reactions that involve LFV include  $\mu^+ \rightarrow e^+ \gamma$  and  $\mu^+ \rightarrow e^+ e^- e^+$ , as well as muon-to-electron conversion in muonic atoms  $\mu^- N \rightarrow e^- N$ . Because muons are abundantly produced at high-intensity proton accelerators and because their simple final states can be very precisely measured, the current best experimental bounds on LFV were obtained on these processes. Prospects for future experimental developments in these rare muon processes also look very promising. A new experiment searching for  $\mu^+ \rightarrow e^+ \gamma$  decays with two orders of magnitude more sensitivity than the previous search is now starting its physics runs in Switzerland. Proposals to search for  $\mu^- N \rightarrow e^- N$  with somewhat better sensitivity than the Swiss-based  $\mu^+ \rightarrow e^+ \gamma$  experiment are now being seriously considered in the United States and Japan. Research and development on a muon storage ring to produce a cleaner and higher-rate muon source are also under way, which could further improve  $\mu^- N \rightarrow e^- N$  sensitivity by another one or two orders of magnitude.

### 2.1. $\mu^+ \rightarrow e^+ \gamma$

Experimentally, a  $\mu^+ \rightarrow e^+ \gamma$  event is characterized by a simple two-body final state: The electron and photon are emitted back to back in the rest frame of the decaying muon, with each carrying away an energy equal to half the muon mass (52.8 MeV), neglecting the tiny electron mass. To utilize this simple but powerful kinematic tool, low-energy muons are stopped in a solid (known as a stopping target). However, in order to avoid formation of muonic atoms that would destroy the two-body kinematic signature, only positive muons are used.

Abundant low-energy positive muons, so-called surface muons (25), are produced by bombarding primary protons into a thick production target. The surface muons come from the decays of positive pions that stop near the surface of the production target and have a sharp momentum spectrum of approximately 29 MeV/c, thanks to two-body decays of the stopped pions. Because of their low momentum and narrow momentum spread (typically 8% FWHM), a thin target ( $\approx 10$  mg cm<sup>-2</sup>) can be employed. Such a low-mass stopping target is essential for minimizing positron annihilations in the target that generate accidental  $\gamma$  ray backgrounds; it is also needed to achieve a good positron momentum resolution, which is critical for suppression of all backgrounds.

Because the surface muons, which come from a stopped pseudoscalar pion decaying via V-A, are naturally 100% spin polarized, the angular distribution of  $\mu^+ \rightarrow e^+ \gamma$  decays can be measured after

discovery of this LFV decay. This distribution may provide important information for helping to pin down the source of the LFV. Researchers have also proposed to reduce backgrounds by limiting the experimental acceptance, as the background positrons and  $\gamma$  rays have angular distributions with respect to the muon spin (26).

The present best upper limit on the branching ratio of  $\mathcal{B}(\mu^+ \rightarrow e^+\gamma)$  is  $1.2 \times 10^{-11}$  (90% CL) (shown in **Table 1**), which was established by the MEGA (Muon decays to an Electron and a GAMMA ray) experiment at the Los Alamos Meson Physics Facility (LAMPF) (27, 28). The major background in a  $\mu^+ \rightarrow e^+\gamma$  search is an accidental coincidence of a positron from the standard Michel decays of muons,  $\mu \rightarrow e\nu\bar{\nu}$ , and a relatively high energy  $\gamma$  ray from radiative muon decays or annihilation of positrons in material. The physics background from radiative muon decays,  $\mu \rightarrow e\nu\bar{\nu}\gamma$  with very low energy neutrinos, on the other hand, is strongly suppressed by reasonably good energy and momentum measurements at a rate more than an order of magnitude smaller than the accidental background.

Because the accidental background increases quadratically with the muon rate, a continuous dc muon beam with the lowest instantaneous rate is better suited for a  $\mu^+ \rightarrow e^+\gamma$  search than a pulsed muon beam. In order to achieve a  $\mathcal{B}(\mu^+ \rightarrow e^+\gamma)$  sensitivity of  $10^{-13}$  in one year of running ( $T \approx 10^7$  s), assuming a detection efficiency of  $\varepsilon \approx 10\%$ , a dc muon rate of  $1/(10^{-13}\varepsilon T) \approx 10^7\text{s}^{-1}$  is needed.

Currently there is only one accelerator in the world that is able to provide such a high-rate dc muon beam: the 590-MeV isochronous ring cyclotron at PSI, in Villigen, Switzerland (near Zurich). The cyclotron constantly supplies a 2.0-mA proton beam with 50 MHz rf time structure. Because the 2- $\mu\text{s}$  muon lifetime is much longer than the rf structure, the muon decay rate has no time structure. The cyclotron is currently being upgraded: Its beam current is planned to reach 2.6 mA in one to two years and 3.0 mA some years thereafter. Eventually, the cyclotron will reach an unrivaled beam power exceeding 1.5 MW.

In 1999, a proposal by a group of Japanese physicists to search for  $\mu^+ \rightarrow e^+\gamma$  decays was approved by PSI's research committee (29, 30). The experimental collaboration has since evolved to approximately 60 physicists from Japan, Switzerland, Italy, Russia, and the United States and is now known as the MEG (Muon to Electron and Gamma) collaboration. It is currently starting physics runs with a sensitivity of  $10^{-13}$ ; with detector upgrades, its sensitivity will eventually reach  $10^{-14}$ . MEG has a clear advantage over the previous MEGA experiment, which used the pulsed LAMPF beam with a macro duty cycle of 7.7% and an instantaneous muon rate of  $2.5 \times 10^8\text{s}^{-1}$ . MEG's dc muon rate is only  $3.0 \times 10^7\text{s}^{-1}$ , resulting in suppression of accidental background by a factor of almost an order of magnitude.

A schematic of the experimental setup of the MEG experiment is shown in **Figure 3**. The main features of the experiment are a novel positron spectrometer with a specially graded magnetic field and an innovative 900- $\ell$  liquid xenon  $\gamma$  ray detector.

The magnetic field of the positron spectrometer COBRA (Constant Bending Radius) (31) varies from 1.27 T at the center to 0.49 T at both ends. It is designed to quickly sweep away positrons from the drift chamber volume while providing a constant projected bending radius for the trajectory of the 52.8-MeV positrons. This significantly reduces the hit rates in the drift chambers and simplifies the positron tracking.

In the liquid xenon detector (32) (shown in **Figure 4**), the scintillation photons caused by an incident  $\gamma$  ray are viewed from all sides by 846 photomultiplier tubes to make a precise measurement of the conversion point, timing, and energy of the  $\gamma$  ray. To identify and separate pileup  $\gamma$  rays efficiently, fast waveform digitizers are used for all the photomultiplier tube outputs (33). Possible impurities (mostly water) that absorb scintillation light are eliminated by circulating liquid xenon through a purification system (34, 35). Stability monitoring and precise calibration of

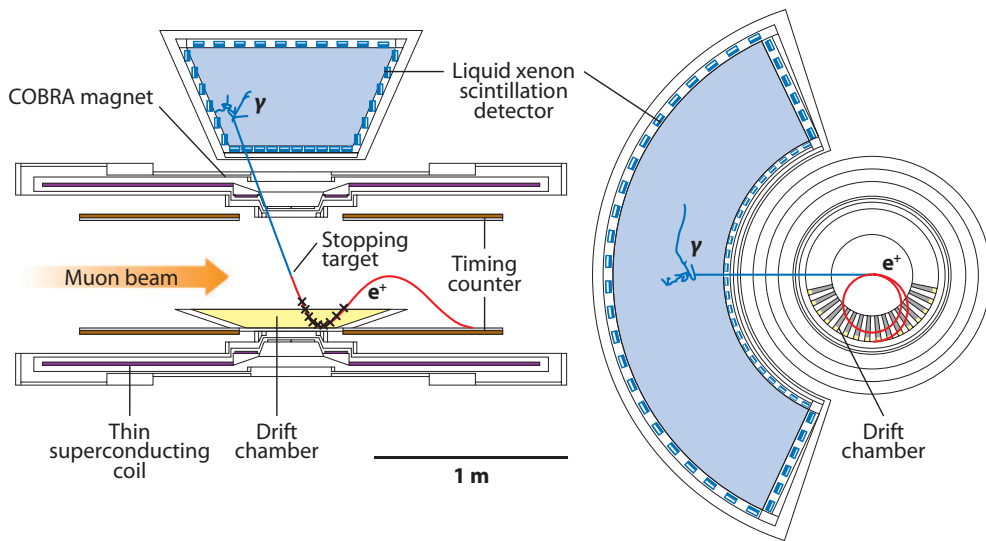


**Figure 3**

Schematic layout of the Muon to Electron and Gamma (MEG) experiment. Used with permission of the MEG Collaboration.

the liquid xenon detector are key to the success of the experiment. Point-like  $^{241}\text{Am}$   $\alpha$  sources deposited on wires (36) and the  $^7\text{Li}(p, \gamma)^8\text{Be}$  reaction provided by a Cockcroft-Walton proton accelerator are used for frequent monitoring and calibration, while 55-MeV  $\gamma$  rays from the pion charge exchange reaction  $\pi^-p \rightarrow \pi^0n$  provide the absolute energy calibration.

It is expected that MEG will reach a 90%-CL expected upper limit sensitivity of  $1 - 2 \times 10^{-13}$  in two to three years. Possible detector upgrades to maximize the available beam intensity,  $1 \times 10^8$  muons  $\text{s}^{-1}$ , which may further increase with the accelerator upgrade, are being investigated; researchers aim to achieve a  $10^{-14}$  sensitivity.

As no accelerator facility has a higher intensity dc muon beam than PSI, and as there are presently no innovative ideas for experiments to make use of such a high-intensity beam, it seems unlikely that any experiment will exceed  $10^{-14}$  in a  $\mu^+ \rightarrow e^+\gamma$  search in the foreseeable future.



**Figure 4**

Photograph of the inside of the Muon to Electron and Gamma (MEG) liquid xenon photon detector as photomultiplier tubes are assembled. Used with permission of the MEG Collaboration.

## 2.2. $\mu^\pm \rightarrow e^\pm e^+ e^-$

Just as in  $\mu^+ \rightarrow e^+ \gamma$  experiments, searches for the  $\mu^+ \rightarrow e^+ e^- e^+$  decay require positive muons to avoid muonic atom formation. With three particles in the final state, these searches also suffer from accidental coincidences: Michel positrons from normal muon decays coincide with  $e^+ e^-$  pairs from  $\gamma$  ray conversions or from Bhabha scattering of Michel positrons with atomic electrons. To minimize accidental background, a dc muon beam should be used.

The present upper limit on the branching ratio,  $1.0 \times 10^{-12}$  (37), was obtained by the SINDRUM experiment (38) in 1988. The SINDRUM collaboration used a subsurface dc muon beam of 25 MeV/c with a rate of  $6 \times 10^6$  muons  $s^{-1}$ . Their spectrometer accepted 24% of  $\mu^+ \rightarrow e^+ e^- e^+$  assuming a flat transition matrix element, with an 18-MeV/c threshold for transverse momentum.

With the presently available beam intensity of  $1 \times 10^8$  muons  $s^{-1}$  at PSI, improvement in sensitivity by one to two orders of magnitude ( $10^{-13} - 10^{-14}$ ) might be possible. Because the background increases linearly with the muon rate squared, background reduction must improve by more than two orders of magnitude. The rather modest tracking performance of SINDRUM in momentum resolution (10% FWHM) and vertex constraints seems to leave enough room for improvements. The most significant issue is whether good tracking devices that work at such high rates ( $10^8 s^{-1}$ ) can be developed. The COBRA spectrometer of the MEG experiment, which focuses only on the highest end of the Michel spectrum, is certainly not suitable for this purpose.

In order to be highly competitive with  $\mu^+ \rightarrow e^+ \gamma$  and  $\mu^- N \rightarrow e^- N$  searches, an experimental sensitivity down to some  $10^{-16}$  is desirable. This would require a dc muon beam of  $10^{10}$  muons  $s^{-1}$ , i.e., a new muon facility with an intensity 100 times higher than that of PSI. From an experimental perspective, tracking at such high rates remains a daunting challenge.

## 2.3. $\mu - e$ Conversion

In muon-to-electron conversion,  $\mu^- N \rightarrow e^- N$ , a muon converts to an electron by exchanging a virtual photon (or undergoes a nonelectromagnetic interaction) with the capture nucleus. As introduced in Section 1.1 and Equation 2, the experimental signature is simple: a single monochromatic electron with  $E_{\text{mec}}$  (105.1 MeV for Al target). Because the method requires the formation of muonic atoms with target nuclei, only negative muons can be used. Moreover, the atomic number dependence of the  $\mu \rightarrow e$  conversion rate can be used to distinguish various theoretical models of LFV after its discovery (20).

As discussed in Section 1.2, for generic chiral-changing dipole photonic vertices that violate lepton flavor, the physics sensitivity of  $\mu^- N \rightarrow e^- N$  is two orders of magnitude lower than that of  $\mu^+ \rightarrow e^+ \gamma$ :  $\frac{1}{389}$  for Al target,  $\frac{1}{238}$  for Ti, and  $\frac{1}{342}$  for Pb in terms of branching ratios (19, 20). Thus, for LFV electromagnetic transitions a  $\mu^+ \rightarrow e^+ \gamma$  branching ratio of  $1 \times 10^{-13}$  corresponds to approximately  $3 \times 10^{-16}$  for  $\mu^- N \rightarrow e^- N$ . To achieve this sensitivity, a negative muon beam with an intensity of  $10^{10} - 10^{11} s^{-1}$  is necessary.

Obtaining such a high muon rate is a major challenge. Because there is no surface muon beam for negative muons, such a high-intensity beam tends to have a much broader spectrum and is usually contaminated by various other particles, particularly pions.

Major backgrounds in a  $\mu^- N \rightarrow e^- N$  search are (a) electrons from muon decays in orbit and (b) beam-related background. The energy  $E_e$  of the decay-in-orbit electron has a spectrum falling off rapidly as  $(E_{\text{mec}} - E_e)^5$ . By improving the electron energy resolution  $\sigma_{E_e}$ , this background decreases as  $\sigma_{E_e}^5$ . Because the energy resolution is dominated by energy loss in the stopping target, a thinner target is required. To efficiently stop a broad spectrum of muons, several layers of thin targets are usually used.

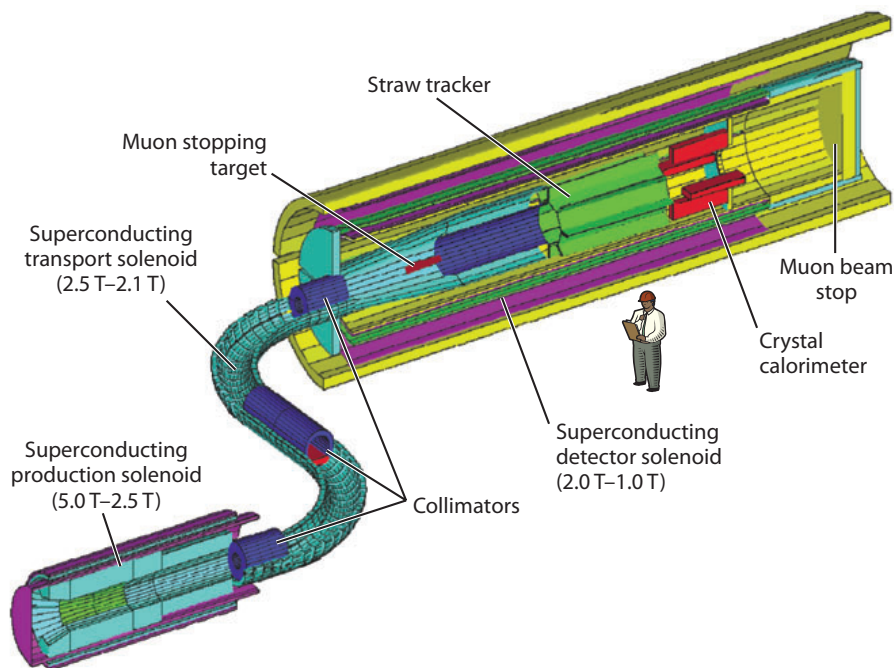


**Figure 5**

Layout of the Muon Electron Conversion (MECO) experiment. Used with permission of proponents of MECO.

There are various beam-related backgrounds caused by beam contaminants, specifically pions. The most significant of these is radiative pion capture, wherein pions may be radiatively captured by the target nuclei, emitting  $\gamma$  rays that subsequently convert into electrons.

The SINDRUM II experiment at PSI, which has set the most stringent upper limits of  $7 \times 10^{-13}$  on  $\mu^- \text{Au} \rightarrow e^- \text{Au}$  (15), has reduced the pion contamination with an 8-mm-thick  $\text{CH}_2$  moderator for a 52-MeV/c beam, where pions have half the range of muons. The main background arises from electrons from radiative pion capture in the degrader or pion decays in flight, which scatter in the target to mimic the signal. They show a time correlation with the cyclotron rf time structure and are thus separated.

The MECO (Muon Electron Conversion) experiment (39) was proposed at Brookhaven National Laboratory to search for  $\mu^- \text{Al} \rightarrow e^- \text{Al}$  at a sensitivity below  $10^{-16}$ . Its schematic layout is shown in **Figure 5**. The experimental design of MECO is based on three key concepts:

1. The use of a graded-field solenoid to collect pions, which leads to a 1000-fold increase in muon intensity (to  $10^{11} \text{ s}^{-1}$ ) over the previous experiment. This idea was originally proposed for a Russian experiment at the Moscow Meson Factory (40).
2. A short-pulsed proton beam extracted with a time interval that matches the muon capture lifetime (approximately  $0.9 \mu\text{s}$  for Al target). To avoid beam-related background, data are taken in a delayed time window after the beam pulse, when all the backgrounds have fallen off. No proton should exist during the delayed time window at the level of  $10^{-9}$  (beam extinction).
3. A curved solenoid selects and transports the low-energy negative muons to the stopping targets with a high transmission probability.

To stop a broad spectrum of muons, 17 layers of 0.2-mm-thick Al targets are used. Al is chosen as the target material because its muon capture lifetime ( $0.9 \mu\text{s}$ ) matches the measurement cycle, whereas heavier elements have much shorter lifetimes.

Unfortunately, MECO was cancelled in 2005 because of budget constraints. However, its importance for physics is still strong. MECO-type experiments are under way both at Fermi National Laboratory (FNAL) and at Japan Proton Accelerator Research Complex (J-PARC). It is expected that minor modifications to the existing accelerators or the accelerators under construction will produce a proton beam with the required structure. The Letter of Intent for the FNAL experiment, Mu2e (41), was submitted in 2007 as was the J-PARC proposal, COMET (42). There is hope that either or both of these experiments may start running soon after the MEG experiment draws to a close.

An ambitious future project is PRISM (Phase-Rotated Intense Slow Muons) (43), designed to produce a high-intensity muon beam with narrow energy spread and low levels of contamination. It is proposed to be built at the J-PARC main proton ring currently under construction at Tokai, Japan. Its schematic layout is shown in **Figure 6**. A fixed-field alternating gradient (FFAG) synchrotron is used to carry out phase rotation, i.e., conversion of an original short-pulse beam with wide momentum spread ( $\pm 30\%$ ) into a long-pulse beam with narrow momentum spread ( $\pm 3\%$ )

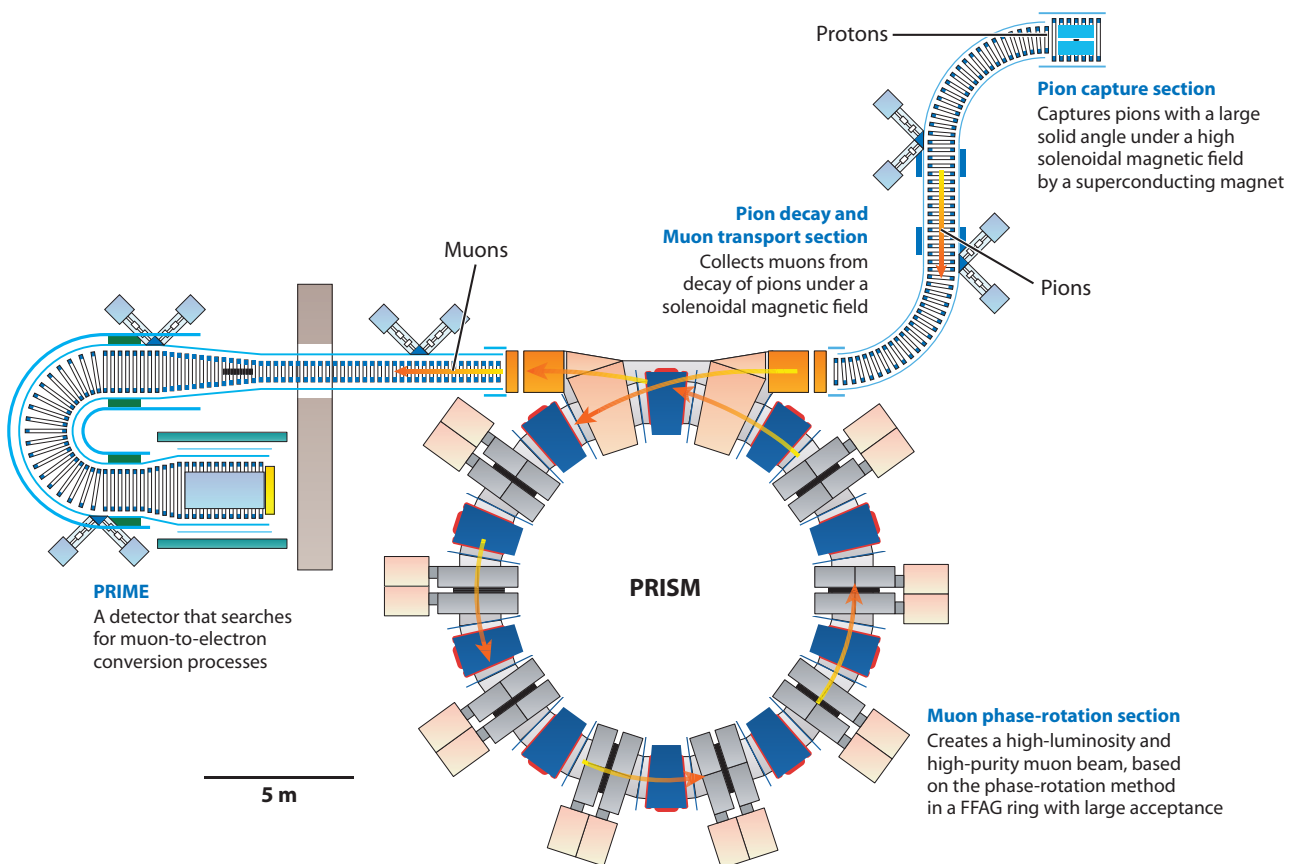


**Figure 6**

A schematic layout of the Phase-Rotated Intense Slow Muons (PRISM) project. Not drawn to scale. Abbreviations: FFAG, fixed-field alternating gradient; PRIME, PRISM Mu E. Used with permission of proponents of PRISM.

by a strong rf field. After five turns in the FFAG ring for the phase rotation, pions in the beam will decay out. Given  $10^{14}$  protons  $s^{-1}$  from the J-PARC ring, the PRISM facility should be able to provide  $10^{11}$ – $10^{12}$  muons  $s^{-1}$ .

PRIME (PRISM Mu E) (43) is a proposed experiment intended to search for  $\mu^- N \rightarrow e^- N$  conversion at the future PRISM facility. Because of a very low duty factor of the PRISM beam, this experiment must handle the extremely high instantaneous rate of  $10^{10}$ – $10^{11}$  muons per beam bunch. In the PRIME experiment, a curved solenoid spectrometer will be used to transport only electrons with desired momenta from the stopping target to the detector. Thanks to the high-quality muon beam at PRISM, which has a high efficiency and a better momentum resolution, we can expect sensitivity of the level of  $10^{-18}$ .

### 3. LEPTON FLAVOR VIOLATION IN TAU LEPTON DECAYS

It is by incorporating results from many different measurements that we will finally be able to move beyond the standard model. Progress will be made by interpreting within a cohesive theoretical framework the variety of results from, for example, direct searches (and discoveries) of new particles at the energy frontier of the Large Hadron Collider (LHC), neutrino oscillation measurements, and  $g$ -2 and electric dipole moment measurements, as well as searches (and discoveries) of LFV in the decays of leptons and mesons. LHC discoveries alone will be insufficient to determine the underlying theoretical structures responsible for new physics. Similarly, a discovery of  $\mu^+ \rightarrow e^+ \gamma$  alone will not provide sufficient information to determine the underlying LFV mechanism or even to identify an underlying theory. Nor do we know which LFV decay mode will first be discovered; therefore, it is critical to probe all LFV modes. Consequently, the  $\mu^+ \rightarrow e^+ \gamma$  search should be augmented by studies of  $\tau^\pm \rightarrow \mu^\pm \gamma$  as well as  $\tau^\pm \rightarrow e^\pm \gamma$ . For example, even in the presence of the existing and projected  $\mu^+ \rightarrow e^+ \gamma$  bounds,  $\tau^\pm \rightarrow \mu^\pm \gamma$  decays are predicted to occur at rates that are accessible at current experiments in many models (44). Moreover, the full set of measurements of  $\mu$  and  $\tau$  LFV processes are required because, in general, there are strong correlations in many models between the expected rates of the various channels. For instance, in a supersymmetric seesaw model describing potential LFV (45, 46), there is an expectation that the specific relative rates of  $\mathcal{B}(\tau^\pm \rightarrow \mu^\pm \gamma) : \mathcal{B}(\tau^\pm \rightarrow \mu^\pm \mu^+ \mu^-) : \mathcal{B}(\tau^\pm \rightarrow \mu^\pm \eta)$  depend upon the model parameters (45, 46). A detailed analysis of the  $\mu$ - $\tau$  LFV in the unconstrained minimal supersymmetric model (MSSM) framework includes a discussion of various correlations and demonstrates that  $\tau$  LFV branching fractions can be as high as  $10^{-7}$  (47), even with the strong experimental bounds on muon LFV. Correlations in a constrained MSSM model (48), indicated in **Figure 7**, also illustrate the complementarity of the  $\mathcal{B}(\tau^\pm \rightarrow \mu^\pm \gamma)$  and  $\mathcal{B}(\mu^+ \rightarrow e^+ \gamma)$  measurements.

#### 3.1. Tau Lepton Data Samples and Search Strategies

Historically,  $\tau$  lepton samples large enough to be useful for searches for LFV have been pair-produced in  $e^+e^-$  storage ring colliders via the process  $e^+e^- \rightarrow \tau^+\tau^-$  operating at a center-of-mass energy near the mass of the  $\Upsilon(4S)$  meson (10.58 GeV). This is because the  $e^+e^-$  colliders optimized for studying  $B$  meson physics and/or CP violation in the  $B$  meson system require the highest luminosities possible at the  $\Upsilon(4S)$  resonance, which decays almost exclusively to a  $B\bar{B}$  pair. These  $B$  factories are in fact  $\tau$  factories as well, as they provide similarly sized  $B\bar{B}$  and  $\tau^+\tau^-$  samples.

In recent years the BaBar and Belle experiments have provided new results on LFV in  $\tau$  decays. Belle, at the Japanese Koo Enerugii Kasokuki Kenkyuu Kikoo (KEKB)  $e^+e^-$  collider, and BaBar, at Stanford Linear Accelerator Center's  $e^+e^-$  Positron Electron Project (PEP-II)  $B$  factory, have

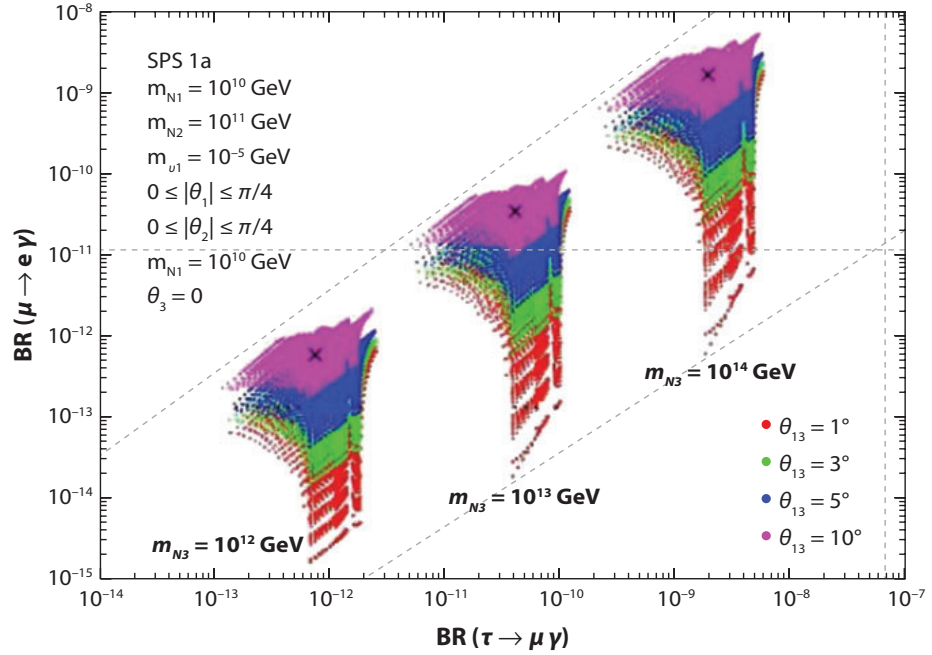


**Figure 7**

$\mathcal{B}(\mu^+ \rightarrow e^+ \gamma)$  versus  $\mathcal{B}(\tau^\pm \rightarrow \mu^\pm \gamma)$  in a constrained minimal supersymmetric model (MSSM) with three right-handed massive neutrinos for three values of the heaviest right-handed neutrino,  $m_{N_3}$ , and four values of  $\theta_{13}$ , for a particular choice of model parameters (48). Used with permission of the authors.

been collecting data at the  $\Upsilon(4S)$  since 1999. PEP-II ceased operations in 2008, whereas KEKB's operations will pause for three or four years beginning in 2009 or later in order to implement an upgrade to higher luminosity. The time-dependent B meson CP violation studies require the beams to have different energies in order to introduce a time dilation from the Lorentz boost. This does not affect the measurements involving the  $\tau$ , but it is an effect that must be taken into account in the analyses. The BaBar (49) and Belle (50) detectors are remarkably similar; the only major difference pertains to the technology used to identify charged particles. Belle uses a threshold Cherenkov detector together with time of flight and tracker  $dE/dx$  (see **Figure 8** for a schematic), whereas BaBar mainly relies on a ring-imaging Cherenkov detector augmented by  $dE/dx$  in the trackers. With more than  $1 \text{ ab}^{-1}$  of data currently being collected between the two experiments and the  $e^+e^- \rightarrow \tau^+\tau^-$  cross section being  $0.919 \text{ nb}$  (51), the world sample of  $\tau$  leptons produced at the  $e^+e^-$  colliders now exceeds  $10^9$ , which allows for experimental probing of LFV processes at the  $\mathcal{O}(10^{-7})$  to  $\mathcal{O}(10^{-8})$  levels.

The general approach of the analyses is to select  $\tau$  pair events with the appropriate charged-particle topology, removing non- $\tau$  events with as minimal an impact as possible on the signal efficiency. This is accomplished by dividing the candidate event into hemispheres in the center of mass, where each hemisphere contains either the  $\tau^+$  or the  $\tau^-$  decay products. Each hemisphere is then considered a possible candidate for the LFV decay under consideration. This can be seen in the BaBar detector's display of a simulated  $e^+e^- \rightarrow \tau^+\tau^-$ ;  $\tau^+ \rightarrow e^+\bar{\nu}_e\nu_e$ ;  $\tau^- \rightarrow \mu^-\gamma$  event (depicted in **Figure 9**). Unlike standard model  $\tau$  decays, which have at least one neutrino, the LFV decay products have a combined energy  $E_{\ell X}$  equal to the energy of the  $\tau$ . This energy is approximately equal to the beam energy in the center of mass,  $\sqrt{s}/2$ , and the decay products' mass ( $m_{\ell X}$ ) is equal to that of the  $\tau$ . A two-dimensional signal region in the  $m_{\ell X}$  versus  $\Delta E$  plane

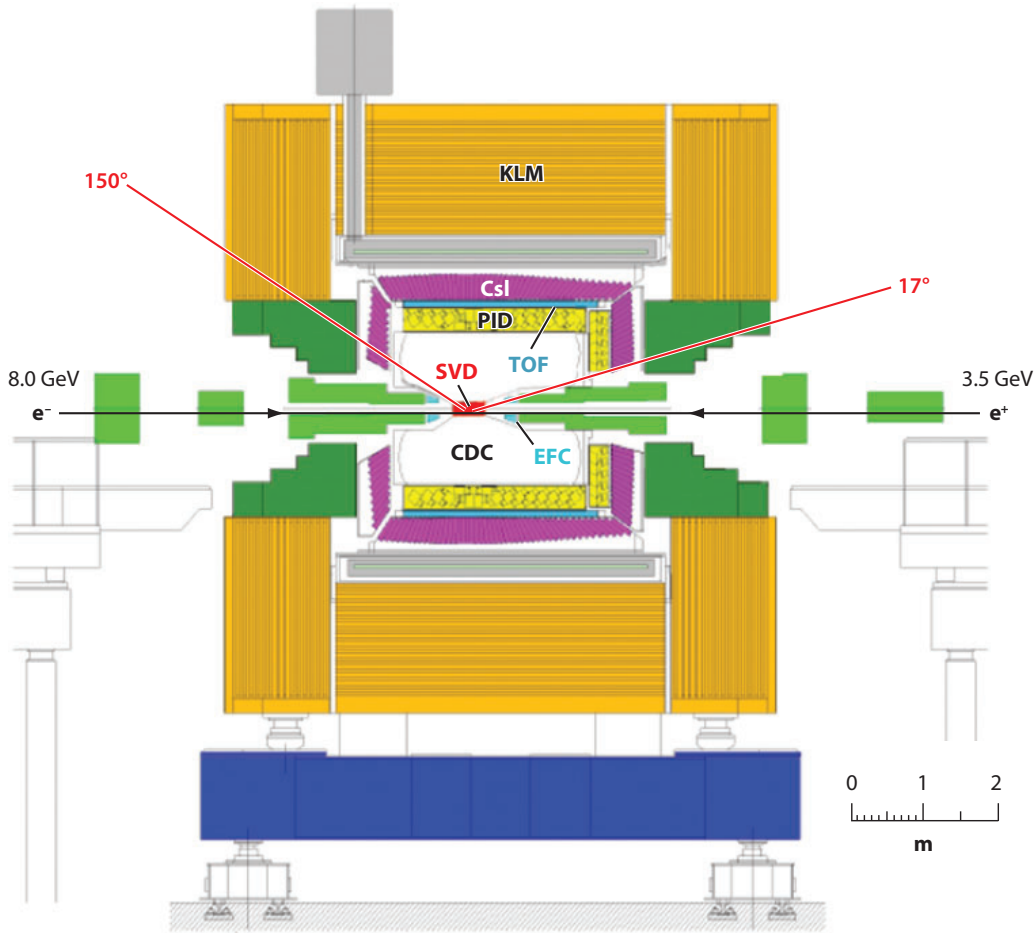


**Figure 8**

Schematic of the Belle detector. Abbreviations: CDC, central drift chamber; CsI, thallium-doped cesium iodide crystal calorimeter; EFC, extreme forward calorimeter; KLM,  $K_L^0$  detection and muon identification; PID, particle identification system; SVD, silicon vertex detector; TOF, time of flight. Used with permission of the Belle Collaboration.

is therefore used to separate the signal from the standard model  $\tau$  decay backgrounds, where  $\Delta E = E_{\ell X} - \sqrt{s}/2$ . **Figure 10** shows the distribution in that plane for simulated  $\tau^\pm \rightarrow \mu^\pm \gamma$  decays, where the peaking at  $\Delta E = 0$  and  $m_{\ell X} = m_\tau = 1777 \text{ MeV}/c^2$  is evident. A signal box in the  $\Delta E$ - $m_{\ell X}$  encompassing events within approximately two standard deviations of  $\Delta E = 0$  and  $m_{\ell X} = m_\tau = 1777 \text{ MeV}/c^2$  is often defined and serves as the most powerful requirement in the searches for LFV in  $\tau$  decay.

Typically the analyses are optimized using Monte Carlo simulations of the signal and backgrounds to give the best-expected upper limit. The simulation of the signal provides the signal efficiency  $\varepsilon$ , which typically lies between 2% and 10% depending on the channel under study. The efficiency components of a generic  $\tau$  LFV decay selection are (roughly) as follows: trigger (90%), acceptance/reconstruction (70%), charged-particle hemisphere topology (1 versus 1 or 1 versus 3: 70%), particle identification (50%), requirements apart from those on  $\Delta E$  and  $m_{\ell X}$  (50%),  $\Delta E$  versus  $m_{\ell X}$  signal box requirements (50%).

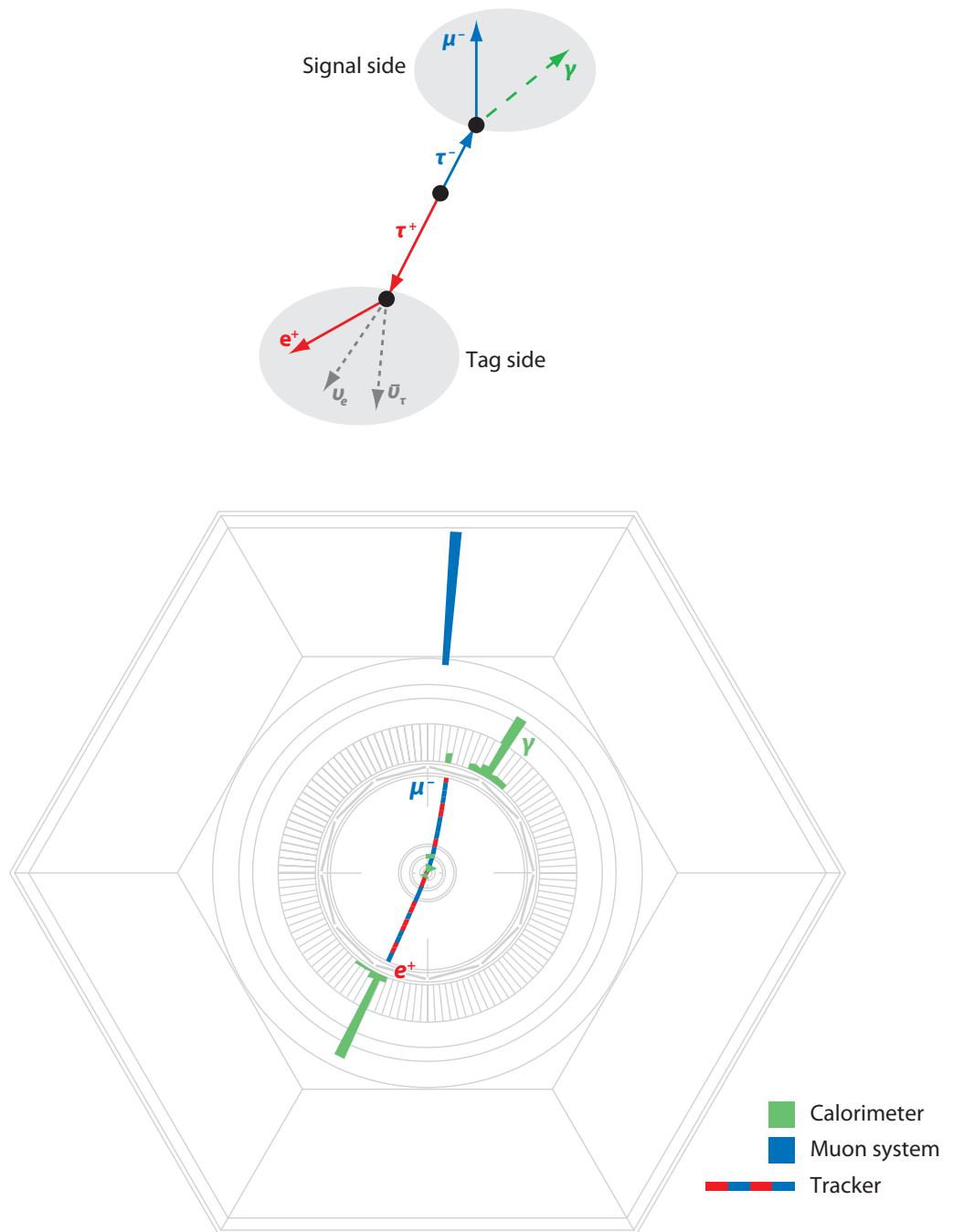


**Figure 9**

Simulated BaBar event display with a lepton flavor violation  $\tau^- \rightarrow \mu^- \gamma$  decay opposite a standard model  $\tau^+ \rightarrow e^+ \bar{\nu}_\tau \nu_e$  decay. Tau leptons decay inside the beam pipe. Used with permission of the Babar Collaboration.

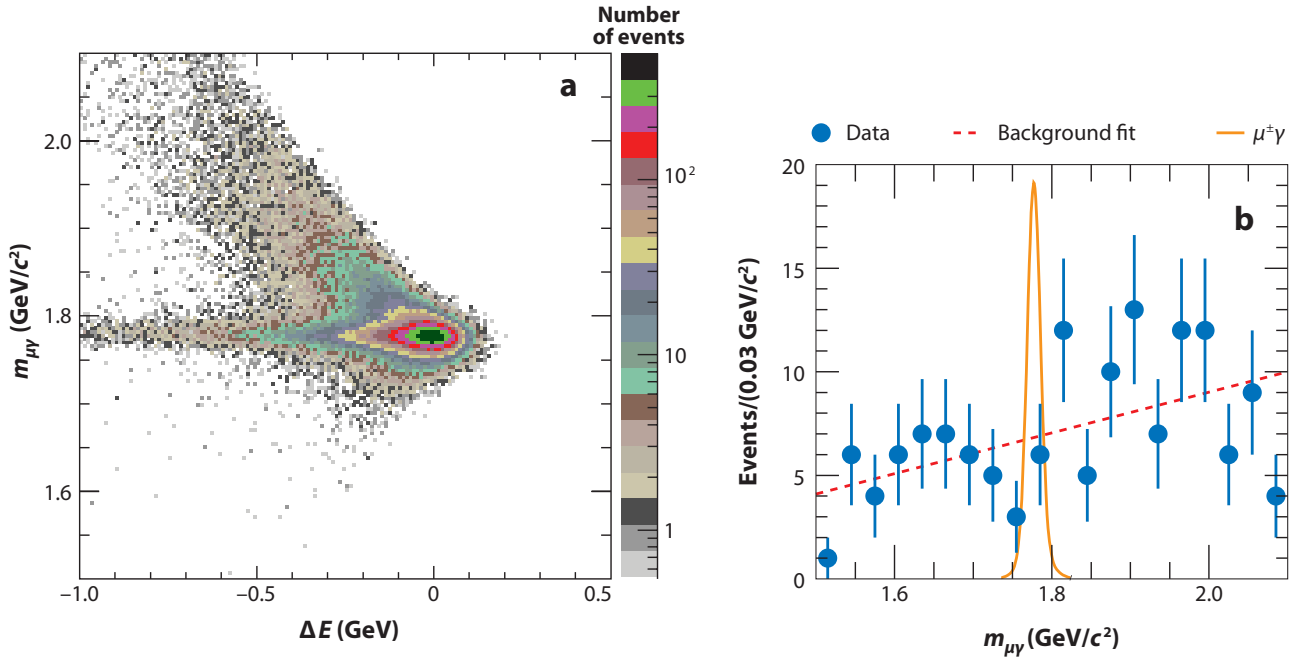


**Figure 10**

(a) The distribution in the  $m_{\mu\gamma}$  versus  $\Delta E$  plane for simulated signal events in the BaBar  $\tau^\pm \rightarrow \mu^\pm\gamma$  analysis. (b) Distribution of BaBar  $m_{\mu\gamma}$  data within a  $2\sigma$  window in  $\Delta E$  (52). Used with permission of the BaBar Collaboration.

The expected number of background events ( $N_{\text{bkd}}$ ) is normally estimated using the distribution shapes from the Monte Carlo simulation of backgrounds with the normalization obtained from the data in the regions outside the signal box. These analyses are blind in the sense that the physics analysts have no knowledge of the data in the signal region when the optimization and systematic studies are undertaken. Once these steps are completed, the data in the signal region is unblinded and the analyst learns the number of events observed in the signal region ( $N_{\text{obs}}$ ). The analyst thus either makes a discovery or—as has been the case to date—sets an upper limit on the process.

$N_{\text{obs}}$  together with  $N_{\text{bkd}}$  then gives the number of signal events,  $N_{\text{sig}}$ : If  $N_{\text{obs}} - N_{\text{bkd}}$  is consistent with zero, an upper limit on  $N_{\text{sig}}$  ( $N_{90}^{\text{UL}}$ ) is established. Schematically, the 90%-CL branching ratio upper limit is obtained from

$$\mathcal{B}_{90}^{\text{UL}} = \frac{N_{90}^{\text{UL}}}{2N_{\tau\tau}\varepsilon} = \frac{N_{90}^{\text{UL}}}{2\mathcal{L}\sigma_{\tau\tau}\varepsilon}, \quad 23.$$

where  $N_{\tau\tau} = \mathcal{L}\sigma_{\tau\tau}$  is the number of  $\tau$  pairs produced in  $e^+e^-$  collisions obtained from the integrated luminosity  $\mathcal{L}$  and from the  $\tau$  pair production cross section  $\sigma_{\tau\tau}$ . In practice, if  $N_{\text{bkd}}$  is more than a few events, then  $N_{\text{sig}}$  and  $N_{\text{bkd}}$  are determined from a fit.

### 3.2. Current Results on Lepton Flavor Violation Decays of the Tau

Experimentally, LFV  $\tau$  decays can be conveniently classified as  $\tau^\pm \rightarrow \ell^\pm\gamma$ ,  $\tau^\pm \rightarrow \ell_1^\pm\ell_2^+\ell_3^-$ , and  $\tau^\pm \rightarrow \ell^\pm b^0$ , where  $\ell$  is either an electron or a muon and where  $b^0$  represents a hadronic system. In the searches by BaBar and Belle, the  $b^0$  has been categorized in three ways: (a)  $b^0$  corresponds to a pseudoscalar meson (e.g.,  $\pi^0$ ,  $\eta$ ,  $\eta'$ ,  $K_S^0$ ); (b)  $b^0$  corresponds to a neutral vector meson

(e.g.,  $\omega$ ,  $K^*(892)$ ,  $\phi$ ); and (c)  $b^0$  is a pair of oppositely charged mesons,  $b^0 = b_1^+ b_2^-$ , where  $b_{1(2)}^\pm = \pi^\pm$  or  $K^\pm$ .

The most recent  $\tau^\pm \rightarrow \mu^\pm \gamma$  and  $\tau^\pm \rightarrow e^\pm \gamma$  results, as yet unpublished, were reported by Belle (53) using a data sample with an integrated luminosity of  $535 \text{ fb}^{-1}$  that corresponds to  $492 \times 10^6$   $\tau$  pair events. The main  $\tau^\pm \rightarrow \mu^\pm \gamma$  backgrounds in these searches arise from  $e^+ e^- \rightarrow \mu^+ \mu^- \gamma$  events and  $e^+ e^- \rightarrow \tau^+ \tau^- \gamma$  events, where one of the  $\tau$ s decays via  $\tau \rightarrow \mu \nu \bar{\nu}$ . In both cases the photon, from initial-state radiation in the latter case and initial- or final-state radiation in the former, combines with a muon to accidentally fall within the signal box. The  $e^+ e^- \rightarrow \tau^+ \tau^- \gamma$ ;  $\tau \rightarrow \mu \nu \bar{\nu}$  events can be classified as irreducible because the events are genuine  $\tau$  pair events and because the  $\mu$  and the  $\gamma$  are correctly identified and measured. A similarly irreducible background source from  $e^+ e^- \rightarrow \tau^+ \tau^- \gamma$ ;  $\tau \rightarrow e \nu \bar{\nu}$  exists. Belle set a 90%-CL upper limit on the number of signal events for  $\tau \rightarrow \mu \gamma$  ( $\tau \rightarrow e \gamma$ ) of 2.0 (3.34) events. These yield upper limits of  $\mathcal{B}(\tau \rightarrow \mu \gamma) < 4.5 \times 10^{-8}$  and  $\mathcal{B}(\tau \rightarrow e \gamma) < 1.2 \times 10^{-7}$ . In 2005, BaBar published 90%-CL upper limits using a  $232\text{-fb}^{-1}$  data sample of  $6.8 \times 10^{-8}$  and  $1.1 \times 10^{-7}$  on  $\mathcal{B}(\tau \rightarrow \mu \gamma)$  and  $\mathcal{B}(\tau \rightarrow e \gamma)$ , respectively (52, 54).

Both experiments report classical frequentist confidence intervals. These are reported in **Table 2**, along with a combined 90%-CL upper limit calculated using both frequentist and Bayesian analyses that take into account correlations and systematic errors. When results from fits are reported, likelihood functions are combined and the  $2 \ln(\Delta \mathcal{L}(\mathcal{B})) = 2.71$  values are used to set the frequentist interval—an approach that reproduces the quoted frequentist intervals of the individual experiments, although both BaBar and Belle use a different approach (55) than that employed here. When event counts in a signal box are reported by both collaborations, the technique of Cousins & Highland (56), following the implementation of Barlow (57), is employed to set a frequentist limit. The Bayesian analysis assumes a prior probability distribution that is uniform in the branching fraction,  $\mathcal{B}$ , and integrates the combined likelihood function from zero to the value of  $\mathcal{B}$  that includes 90% of  $\int_0^\infty \mathcal{L}(\mathcal{B}) d\mathcal{B}$ . Note that when an experiment experiences a downward fluctuation in the background, the reported frequentist interval usually has an upper limit somewhat lower than the Bayesian limit.

Both Belle (58) and BaBar (59) have recently published new results on searches for  $\tau \rightarrow \ell_1 \ell_2 \ell_3$ , but no evidence for a signal was seen by either experiment. Unlike the  $\tau^\pm \rightarrow \mu^\pm \gamma$  and  $\tau^\pm \rightarrow e^\pm \gamma$  searches, there is no irreducible background at the current luminosities. The Belle  $\tau \rightarrow \ell_1 \ell_2 \ell_3$  analysis used  $492 \times 10^6$   $\tau$  pairs, whereas BaBar reported on an analysis using  $346 \times 10^6$

**Table 2** Summary of 90%-CL upper limits on  $\mathcal{B}(\tau \rightarrow \ell \gamma)$  and  $\mathcal{B}(\tau \rightarrow \ell_1 \ell_2 \ell_3)$  LFV  $\tau$  decays<sup>a</sup>

Channel	Belle <sup>b</sup>		BaBar <sup>c</sup>		Combined BF	
	$N_{\text{obs}} (N_{\text{bkg}})$ events	BF ( $10^{-8}$ )	$N_{\text{obs}} (N_{\text{bkg}})$ events	BF ( $10^{-8}$ )	Frequentist ( $10^{-8}$ )	Bayesian ( $10^{-8}$ )
$\tau \rightarrow \mu \gamma$	10 ( $13.9^{+6.0}_{-4.8}$ )	4.5	4 ( $6.2 \pm 0.5$ )	6.8	2.3	5.9
$\tau \rightarrow e \gamma$	5 ( $5.14^{+3.86}_{-2.81}$ )	12	1 ( $1.9 \pm 0.4$ )	11	7.2	8.5
$\tau \rightarrow \mu e^+ e^-$	0 ( $0.04 \pm 0.04$ )	2.7	2 ( $0.89 \pm 0.27$ )	8.0	3.0	3.0
$\tau \rightarrow \mu \mu^+ \mu^-$	0 ( $0.07 \pm 0.05$ )	3.2	0 ( $0.33 \pm 0.19$ )	5.3	1.7	2.0
$\tau \rightarrow e \mu^+ \mu^-$	0 ( $0.05 \pm 0.03$ )	4.1	0 ( $0.81 \pm 0.31$ )	3.7	1.4	2.2
$\tau \rightarrow e e^+ e^-$	0 ( $0.40 \pm 0.30$ )	3.6	1 ( $1.33 \pm 0.25$ )	4.3	1.8	2.6

<sup>a</sup>Belle results are based on  $N_{\tau\tau} = 492 \times 10^6$ , whereas BaBar has published on  $N_{\tau\tau} = 213 \times 10^6$  for the  $\tau \rightarrow \ell \gamma$  and  $N_{\tau\tau} = 346 \times 10^6$  for the  $\tau \rightarrow \ell_1 \ell_2 \ell_3$  results. The combined limits are given in the last two columns. The charge of  $\ell_1$  is equal to the  $\tau$  charge. Both frequentist and Bayesian combinations are reported.

<sup>b</sup>Data from References 53 and 58.

<sup>c</sup>Data from References 52, 54, and 59. Abbreviation: BF, branching fraction.

**Table 3** Summary of 90%-CL upper limits on  $\mathcal{B}(\tau \rightarrow \ell b^0)$  in units of  $(10^{-8})$

Channel	$\ell = e (10^{-8})$				$\ell = \mu (10^{-8})$			
	Belle	BaBar	Combined		Belle	BaBar	Combined	
			Frequentist	Bayesian			Frequentist	Bayesian
$\tau \rightarrow \ell \pi^0$	8	13	4.2	5.0	12	11	5.5	6.4
$\tau \rightarrow \ell \eta$	9.2	16	4.3	6.8	6.5	15	4.9	6.1
$\tau \rightarrow \ell \eta'$	16	24	8.9	9.7	13	14	5.2	7.3
$\tau \rightarrow \ell K_S^0$	5.6		5.6		4.9		4.9	
$\tau \rightarrow \ell \phi$	7.3		7.3		13		13	
$\tau \rightarrow \ell \rho^0$	6.3		6.3		6.8		6.8	
$\tau \rightarrow \ell \omega$	18	10	8.3	8.5	8.9	11	3.4	5.6
$\tau \rightarrow \ell K^{*0}$	7.8		7.8		5.9		5.9	
$\tau \rightarrow \ell \bar{K}^{*0}$	7.7		7.7		10		10	

$\ell = \mu$  or  $e$  and  $b^0$  is either a pseudoscalar (upper four rows) or a vector meson (lower five rows) from the Belle (60, 62, 64) and BaBar (61, 63) experiments. Also listed are their frequentist and Bayesian combinations.

$\tau$  pairs. Note that, in addition to the reactions listed in **Table 2**, the experiments also report bounds of similar magnitude on  $\tau^- \rightarrow e^- \mu^+ e^-$  and  $\tau^- \rightarrow \mu^- e^+ \mu^-$ , which violate lepton flavor twice.

Belle, using  $401 \text{ fb}^{-1}$  (60), and BaBar, using  $339 \text{ fb}^{-1}$  (61), have both published bounds on LFV  $\tau$  decays involving a lepton and a  $\pi^0$ ,  $\eta$ , or  $\eta'$  pseudoscalar. Belle has also published results on searches for  $\tau \rightarrow \ell K_S^0$  (62). Searches for LFV involving the  $\omega$  vector meson,  $\tau \rightarrow \ell \omega$ , have been reported by both experiments, with BaBar employing a data set of  $384 \text{ fb}^{-1}$  (63) and Belle,  $543 \text{ fb}^{-1}$  (64). Using the same data set, Belle has also searched for  $\tau \rightarrow \ell \phi$ ,  $\tau \rightarrow \ell K^{*0}$ , and  $\tau \rightarrow \ell \bar{K}^{*0}$ . The 90%-CL bounds on these processes are typically around  $10^{-7}$  and are listed in **Table 3**. BaBar, using  $221 \text{ fb}^{-1}$ , sets limits on LFV inclusive decays with two charged mesons,  $\tau^\pm \rightarrow \ell^\pm b_1^+ b_2^-$ , where no assumptions are made on the resonance structure of the hadronic final state (65). These bounds range from  $1 \times 10^{-7}$  to  $5 \times 10^{-7}$ , depending on the final state. Belle's equivalent analysis used  $158 \text{ fb}^{-1}$  and set bounds ranging from  $2 \times 10^{-7}$  to  $16 \times 10^{-7}$  (66).

### 3.3. Future Prospects

By the end of 2008, Belle and BaBar will have a combined data sample of roughly  $1.5 \text{ ab}^{-1}$  corresponding to the production of about  $2 \times 10^9$   $\tau$  leptons, and they can be expected to update their analyses using their complete data sets over the following year or two. However, new significantly higher luminosity  $e^+e^-$  colliders operating on or below the  $\Upsilon(4S)$  (67) are on the horizon; these represent exciting new opportunities for the discovery and potential study of LFV decays of the  $\tau$ . One of these colliders is a proposed upgrade of the KEKB facility, which will operate with substantially higher beam currents and which will see luminosities of  $10^{35} \text{ cm}^{-2} \text{ s}^{-1}$  (68). There is also a proposal for a new facility near Frascati, Italy, designed for luminosities of  $10^{36} \text{ cm}^{-2} \text{ s}^{-1}$  (44), or 100 times higher the luminosity of present machines. This increase will be achieved not by increasing the current, but by decreasing the interaction spot size. The higher-luminosity "SuperB" flavor factory would go online a couple of years after the proposed KEKB upgrade, and would yield  $75 \text{ ab}^{-1}$  of data over a five-year period. Such a facility would probe LFV  $\tau^\pm \rightarrow \ell^\pm \ell^+ \ell^-$  and  $\tau^\pm \rightarrow \ell^\pm b^0$  decays, which have no irreducible backgrounds, at the  $\mathcal{O}(10^{-10})$  level. However,

the initial-state photon accidental backgrounds discussed in Section 3.2 will likely prevent the  $\tau^\pm \rightarrow \ell^\pm \gamma$  decays from being probed below the level of a few  $10^{-9}$  for an integrated luminosity of  $75 \text{ ab}^{-1}$ .

Also, very large numbers of  $\tau$  leptons will be produced at the LHC (69) via  $W \rightarrow \tau \bar{\nu}_\tau$  ( $1.7 \times 10^8$ ),  $\gamma/Z^0 \rightarrow \tau^+ \tau^-$  ( $3.2 \times 10^8$ ),  $B \rightarrow \tau X$  ( $7.8 \times 10^{11}$ ),  $B_s \rightarrow \tau X$  ( $7.9 \times 10^{10}$ ), and  $D_s \rightarrow \tau X$  ( $1.5 \times 10^{12}$ ) decays, where the number of such decays per  $10 \text{ fb}^{-1}$  are given in parentheses. The LHC will run for a few years at low luminosity ( $2 \times 10^{33} \text{ cm}^{-2} \text{ s}^{-1}$ ), producing integrated luminosities of  $10\text{--}30 \text{ fb}^{-1}$  of data per year. Subsequently, the collider will run at high luminosity ( $10^{34} \text{ cm}^{-2} \text{ s}^{-1}$ ) for a longer period, collecting between  $100 \text{ fb}^{-1}$  and  $300 \text{ fb}^{-1}$  of data. Simulation studies with ATLAS (A Toroidal LHC Apparatus) and CMS (Compact Muon Selenoid) focusing on  $W^\pm$  and  $Z^0$  production (which are less demanding on trigger thresholds) have concluded that, owing to the hostile background, sensitivities to  $\tau^\pm \rightarrow \mu^\pm \gamma$  are not competitive with existing limits from the B factories (70), even with statistics from one year of high-luminosity running. The situation for  $\tau^\pm \rightarrow \mu^\pm \mu^+ \mu^-$ , although more promising, is still very challenging. With currently planned trigger configurations and  $30 \text{ fb}^{-1}$  of data, expected upper limits from  $W^\pm$ ,  $Z^0$ , and  $B$  meson decays are  $3.8 \times 10^{-8}$ ,  $3.4 \times 10^{-7}$ , and  $2.1 \times 10^{-7}$ , respectively. To fully exploit the huge  $\tau$  production rates and to significantly improve these sensitivities would require the development of new trigger configurations and analysis methods providing access to  $B$  and  $D_s$  production modes under high-luminosity running conditions, which poses a significant challenge to experimenters.

#### 4. SEARCHES FOR CHARGED LEPTON FLAVOR VIOLATION IN MESON DECAYS

In addition to searches for evidence of LFV in the decays of the  $\tau$  and muon as well as in  $\mu$ -e conversion, experiments have searched for LFV in the decays of a variety of charged and neutral pseudoscalar and neutral vector mesons (e.g., pions,  $\eta$ ,  $\eta'$ , kaons,  $D$  mesons,  $B$  mesons,  $J/\psi$ ,  $\Upsilon$ ).

The pseudoscalar meson decays probe  $q \rightarrow q' \ell_1 \ell_2$  transitions and as such are particularly sensitive to lepton-quark models (71). Also, they provide information complementary to the leptonic decay LFV processes, as discussed in Landsberg's recent review (72). The most stringent experimental bounds on mesonic LFV decays are from  $K^+ \rightarrow \pi^+ \mu^+ e^-$  and  $K_L^0 \rightarrow \mu^\pm e^\mp$ , which are bounded at 90% CL to  $1.3 \times 10^{-11}$  (73) and  $4.7 \times 10^{-12}$  (74), respectively. These bounds provide sensitivity to  $s \rightarrow d e \mu$  transitions. Other lepton and  $q$  and  $q'$  combinations in  $q \rightarrow q' \ell_1 \ell_2$  transitions are probed by LFV decays of the  $\pi^0$ ,  $\eta$ ,  $\eta'$ ,  $D^0$ ,  $D^+$ ,  $D_s^+$ ,  $B^0$ , and  $B_s^0$ , along with the  $\tau \rightarrow \ell b^0$  searches, where  $b^0$  is a light pseudoscalar meson. A sample of the bounds on pseudoscalar meson LFV decays is given in **Table 4**.

Similarly, searches for LFV in  $\tau^\pm \rightarrow \ell^\pm b^0$ , where  $b^0$  is a neutral vector meson (e.g.,  $\omega$ ,  $\phi$ ,  $K^{*0}$ ), are particularly sensitive to sources of LFV arising from the exchange of neutral particles that couple to light neutral vector mesons. The LFV source might involve mass-dependent couplings, so it is worthwhile searching for LFV decays of heavier vector mesons. However, few such searches have been undertaken. The notable exceptions are the BES collaboration's searches for  $\mathcal{J}/\psi \rightarrow \mu^\pm e^\mp$  ( $< 1.1 \times 10^{-6}$  at 90% CL),  $\mathcal{J}/\psi \rightarrow \mu^\pm \tau^\mp$  ( $< 2.0 \times 10^{-6}$  at 90% CL), and  $\mathcal{J}/\psi \rightarrow e^\pm \tau^\mp$  ( $< 8.3 \times 10^{-6}$  at 90% CL) (84, 85). Also, the BaBar collaboration has searched for  $e^+ e^- \rightarrow \mu^\pm \tau^\mp$  and  $e^+ e^- \rightarrow e^\pm \tau^\mp$  using  $211 \text{ fb}^{-1}$  at the  $\Upsilon(4S)$  (86). These researchers quote limits on the cross sections of  $\sigma_{\mu\tau} < 3.8 \text{ fb}^{-1}$  and  $\sigma_{e\tau} < 9.2 \text{ fb}^{-1}$  at 90% CL, which we can interpret as bounds on the  $\Upsilon(4S)$  branching fractions of  $\mathcal{B}(\Upsilon \rightarrow \mu^\pm \tau^\mp) < 3.5 \times 10^{-6}$  and  $\mathcal{B}(\Upsilon \rightarrow e^\pm \tau^\mp) < 8.4 \times 10^{-6}$ . Although a complete investigation would in principle require searches for e.g.,  $\omega \rightarrow e^\pm \mu^\mp$ ,  $\phi \rightarrow e^\pm \mu^\mp$ , and  $\Upsilon(nS) \rightarrow e^\pm \mu^\mp$ , the existing limits on  $\mu^\pm \rightarrow e^\pm e^+ e^-$  and  $\mu^- N \rightarrow e^- N$  already greatly constrain such decays.

**Table 4** Bounds at 90% CL on selected lepton flavor violating decays of pseudoscalar mesons

Channel	Upper limit	Experiment	Reference
$\pi^0 \rightarrow \mu^\pm e^\mp$	$3.59 \times 10^{-10}$	KTeV	75
$\eta \rightarrow \mu^\pm e^\mp$	$6 \times 10^{-6}$	Saturne SPES2	76
$K_L^0 \rightarrow \pi^0 \mu^\pm e^\mp$	$7.56 \times 10^{-11}$	KTeV	75
$K_L^0 \rightarrow 2\pi^0 \mu^\pm e^\mp$	$1.64 \times 10^{-10}$	KTeV	75
$K_L^0 \rightarrow \mu^+ e^-$	$4.7 \times 10^{-12}$	BNL E871	74
$K^+ \rightarrow \pi^+ \mu^+ e^-$	$1.3 \times 10^{-11}$	BNL E865, E777	73
$D^+ \rightarrow \pi^+ \mu^\pm e^\mp$	$3.4 \times 10^{-5}$	Fermilab E791	77
$D^+ \rightarrow K^+ \mu^\pm e^\mp$	$6.8 \times 10^{-5}$	Fermilab E791	77
$D^0 \rightarrow \mu^\pm e^\mp$	$8.1 \times 10^{-7}$	BaBar	78
$D_s^+ \rightarrow \pi^+ \mu^\pm e^\mp$	$6.1 \times 10^{-4}$	Fermilab E791	77
$D_s^+ \rightarrow K^+ \mu^\pm e^\mp$	$6.3 \times 10^{-4}$	Fermilab E791	77
$B^0 \rightarrow \mu^\pm e^\mp$	$9.2 \times 10^{-8}$	BaBar (347 fb <sup>-1</sup> )	79
$B^0 \rightarrow \tau^\pm e^\mp$	$1.1 \times 10^{-4}$	CLEO (9.2 fb <sup>-1</sup> )	80
$B^0 \rightarrow \tau^\pm \mu^\mp$	$3.8 \times 10^{-5}$	CLEO (9.2 fb <sup>-1</sup> )	80
$B^+ \rightarrow K^+ e^\pm \mu^\mp$	$9.1 \times 10^{-8}$	BaBar (208 fb <sup>-1</sup> )	81
$B^+ \rightarrow K^+ e^\pm \tau^\mp$	$7.7 \times 10^{-5}$	BaBar (348 fb <sup>-1</sup> )	82
$B_s^0 \rightarrow e^\pm \mu^\mp$	$6.1 \times 10^{-6}$	CDF (102 pb <sup>-1</sup> )	83

Abbreviations: BNL, Brookhaven National Laboratory; CDF, Collider Detector at Fermilab; KTeV, Kaons at the Tevatron.

## 5. SEARCHES FOR CHARGED LEPTON FLAVOR VIOLATION IN $Z^0$ DECAYS

The LFV interactions between charged leptons  $\ell_i^\pm$  and  $\ell_j^\pm$  involving the  $Z^0$  boson can be expressed in the most general way by (87):

$$\begin{aligned} \mathcal{L}_{ij}^{LFV} = & -ig_Z \bar{\ell}_i \gamma^\mu \left[ a_L^{ij} \left( \frac{1-\gamma_5}{2} \right) + a_R^{ij} \left( \frac{1+\gamma_5}{2} \right) \right] Z_\mu \ell_j \\ & + g_Z \bar{\ell}_i \sigma^{\mu\nu} \frac{k_\nu}{M_Z} \left[ b_L^{ij} \left( \frac{1-\gamma_5}{2} \right) + b_R^{ij} \left( \frac{1+\gamma_5}{2} \right) \right] Z_\mu \ell_j + b.c. \end{aligned} \quad (24)$$

where  $g_Z = e/(\sin \theta_W \cos \theta_W)$  is the weak coupling constant,  $k_\nu$  is the  $Z^0$  boson four momentum, and the couplings  $a_L^{ij}$ ,  $a_R^{ij}$ ,  $b_L^{ij}$ , and  $b_R^{ij}$  are not known a priori. The branching fraction ratio of LFV  $Z^0 \rightarrow \ell_i^\pm \ell_j^\mp$  decays to standard model  $Z^0 \rightarrow \mu^+ \mu^-$  decays is

$$\frac{\mathcal{B}(Z^0 \rightarrow \ell_i^\pm \ell_j^\mp)}{\mathcal{B}(Z^0 \rightarrow \mu^+ \mu^-)} = \frac{2 \left( (a_L^{ij})^2 + (a_R^{ij})^2 \right) + (b_L^{ij})^2 + (b_R^{ij})^2}{g_{L\ell}^2 + g_{R\ell}^2}, \quad (25)$$

where  $g_{L\ell}$  and  $g_{R\ell}$  are the left- and right-handed standard model couplings of the  $Z^0$  to muons, respectively. At tree level these couplings have the values  $g_{L\ell}^{tree} = -\frac{1}{2} + \sin^2 \theta_W$  and  $g_{R\ell}^{tree} = \sin^2 \theta_W$ , where  $\sin^2 \theta_W \approx 0.23$ .

The limits on LFV from charged lepton decays can be interpreted as indirect limits on LFV  $Z^0$  decays. However, the  $k_\nu/M_Z$  factor in Equation 24 completely suppresses the sensitivity of the charged lepton decays to  $b_L^{ij}$  and  $b_R^{ij}$ , allowing us only to interpret LFV charged lepton decay limits as bounds on  $(a_L^{ij})^2$  and  $(a_R^{ij})^2$ . For example,  $\mu^\pm \rightarrow e^\pm e^+ e^-$  can be considered to proceed as

$\mu^\pm \rightarrow Z^0 e^\pm, Z^0 \rightarrow e^+e^-$ . In this case (87), we find

$$\frac{\mathcal{B}(\mu^\pm \rightarrow e^\pm e^+ e^-)}{\mathcal{B}(\mu \rightarrow e \nu \bar{\nu})} = 2 \left( 3 \left( (a_L^{e\mu})^2 + (a_R^{e\mu})^2 \right) (g_{L\ell}^2 + g_{R\ell}^2) + \left( (a_L^{e\mu})^2 - (a_R^{e\mu})^2 \right) (g_{L\ell}^2 - g_{R\ell}^2) \right), \quad 26.$$

where the highly suppressed  $b_L^{ij}$  and  $b_R^{ij}$  contributions have been neglected. Using the LEP (Large Electron Positron Collider)– and SLC (Stanford Linear Collider)–measured values for the effective couplings  $g_{L\ell} = -0.26939 \pm 0.00022$  and  $g_{R\ell} = +0.23186 \pm 0.00023$  (88),

$$\frac{\mathcal{B}(\mu^\pm \rightarrow e^\pm e^+ e^-)}{\mathcal{B}(\mu \rightarrow e \nu \bar{\nu})} = 0.7956[(a_L^{e\mu})^2 + 0.9054(a_R^{e\mu})^2]. \quad 27.$$

Therefore, the limit of  $\mathcal{B}(\mu^\pm \rightarrow e^\pm e^+ e^-) < 1.0 \times 10^{-12}$  at 90% CL (37) can be interpreted as a bound:

$$(a_L^{e\mu})^2 + 0.9054(a_R^{e\mu})^2 < 1.3 \times 10^{-12}. \quad 28.$$

We note, however, that the  $b^{ij}$  in Equation 24 are coefficients of chiral-changing operators and therefore are very likely to be suppressed by the factor  $m_\ell/M$ , where  $M$  is a high-mass scale associated with the underlying new physics of LFV. Therefore, assuming that these coefficients are negligible, we find from Equations 25 and 28 that  $\mathcal{B}(Z^0 \rightarrow e^\pm \mu^\mp) < 10^{-12}$ . A similar analysis, using constraints from  $\mu^- N \rightarrow e^- N$ , leads to the even more stringent constraint  $\mathcal{B}(Z^0 \rightarrow e^\pm \mu^\mp) < 10^{-13}$  (89). This bound could be lowered much further as the sensitivity of  $\mu^- N \rightarrow e^- N$  in future experiments improves. These indirect bounds suggest that the observation of the mode  $Z^0 \rightarrow e^\pm \mu^\mp$  at future high-energy colliders (even those capable of producing  $> 10^{10}$   $Z^0$  bosons) is highly unlikely, even though the signature for  $Z^0 \rightarrow e^\pm \mu^\mp$  would be very clean.

Similarly, the limits from LFV in  $\tau$  decays can also be used to bound  $e$ - $\tau$  and  $\mu$ - $\tau$  LFV couplings of the  $Z^0$ . An additional feature that the  $\tau$  decay provides, which is not accessible from muon decays, is individual access to  $(a_L^{e\tau})^2$ ,  $(a_R^{e\tau})^2$ ,  $(a_L^{\mu\tau})^2$ , and  $(a_R^{\mu\tau})^2$ . This access occurs because in the  $\tau^\pm \rightarrow e^\pm \mu^+ \mu^-$  and  $\tau^\pm \rightarrow \mu^\pm e^+ e^-$  decays the  $\mu^+ \mu^-$  and  $e^+ e^-$  pairs are produced via a virtual  $Z^0$  leading to the relationships

$$\frac{\mathcal{B}(\tau^\pm \rightarrow \ell_1^\pm \ell_2^+ \ell_2^-)}{\mathcal{B}(\tau \rightarrow e \nu \bar{\nu})} \equiv R_{\ell_1 \ell_2 \ell_2} = 4 \left( (a_L^{\ell\tau})^2 + (a_R^{\ell\tau})^2 \right) (g_{L\ell}^2 + g_{R\ell}^2), \quad 29.$$

as well as to expressions analogous to Equation 26 for  $\tau^\pm \rightarrow e^\pm e^+ e^-$  and  $\tau^\pm \rightarrow \mu^\pm \mu^+ \mu^-$  decays. From these relations one can set the following limits at 90% CL using the combined Belle and BaBar branching fractions listed in **Table 2**:

$$(a_R^{e\tau})^2 + (a_L^{e\tau})^2 < 1.9 \times 10^{-7}; \quad (a_R^{e\tau})^2 < 2.0 \times 10^{-6}; \quad (a_L^{e\tau})^2 < 1.3 \times 10^{-6} \quad 30.$$

$$(a_R^{\mu\tau})^2 + (a_L^{\mu\tau})^2 < 3.3 \times 10^{-7}; \quad (a_R^{\mu\tau})^2 < 1.3 \times 10^{-6}; \quad (a_L^{\mu\tau})^2 < 3.5 \times 10^{-6}. \quad 31.$$

Again, ignoring the chiral-changing  $b^{ij}$  terms in Equation 24, we find from these constraints the indirect bounds  $\mathcal{B}(Z^0 \rightarrow e^\pm \tau^\mp) < 10^{-7}$  and  $\mathcal{B}(Z^0 \rightarrow \mu^\pm \tau^\mp) < 2 \times 10^{-7}$ .

The most stringent direct limits on  $e\mu$  and  $e\tau$  decays of the  $Z^0$  from a single experiment were provided by OPAL (Omni Purpose Apparatus for LEP) based on the analysis of a data sample of  $5.0 \times 10^6 e^+e^- \rightarrow Z^0$  events, whereas DELPHI (Detector with Lepton, Photon, and Hadron Identification) provided limits for  $\mu$ - $\tau$  decays using  $3.9 \times 10^6 Z^0$  events. The OPAL data yielded 95%-CL upper limits of  $\mathcal{B}(Z^0 \rightarrow e^\pm \mu^\mp) < 1.7 \times 10^{-6}$  and  $\mathcal{B}(Z^0 \rightarrow e^\pm \tau^\mp) < 9.8 \times 10^{-6}$  at 95% CL (90). DELPHI set an upper limit of  $\mathcal{B}(Z^0 \rightarrow \mu^\pm \tau^\mp) < 1.2 \times 10^{-5}$  at 95% CL (91). These limits, together with Equation 25 and Equations 28, 30, and 31, enable us to set 95%-CL bounds on the  $(b_L^{ij})^2 + (b_R^{ij})^2$  couplings of Equation 25:

$$(b_R^{e\mu})^2 + (b_L^{e\mu})^2 < 6.3 \times 10^{-6}; \quad (b_R^{e\tau})^2 + (b_L^{e\tau})^2 < 3.7 \times 10^{-5}; \quad (b_R^{\mu\tau})^2 + (b_L^{\mu\tau})^2 < 4.5 \times 10^{-5}. \quad 32.$$

Alternatively, one can argue (assuming negligible  $b^{ij}$ ) that the indirect bounds on  $Z^0 \rightarrow e^\pm \tau^\mp$  and  $Z^0 \rightarrow \mu^\pm \tau^\mp$  are currently about two orders of magnitude more stringent than the direct  $Z^0$  decay constraints and that those indirect bounds will be further reduced as the sensitivity of rare  $\tau$  decays improves. Again, it seems that observation of the LFV decays  $Z^0$  into  $e\tau$  or  $\mu\tau$  is highly unlikely. The above  $Z^0$  decay exercise illustrates a nice complementarity between high-energy collider searches for LFV and lower-energy LFV constraints from muon and  $\tau$  decay studies. The latter studies are already very stringent and will continue to improve. If an LFV signal is observed at a high-energy collider, any attempt to explain it as underlying new physics must confront the tight constraints arising from rare muon and  $\tau$  processes.

## 6. SUMMARY AND OUTLOOK

Historically, searches for charged lepton flavor violation have had an enormous impact on the development of particle physics in spite of the fact that no violation of lepton flavor involving charged leptons has ever been observed. In recent years, the BaBar and Belle experiments have reduced the bounds on third-generation LFV by two orders of magnitude over previous measurements, and plans for SuperB flavor factories on the horizon will see the experiments reach  $10^{-9}$ – $10^{-10}$  levels. Meanwhile, we look forward to seeing what MEG has in store over the next year or two as it reaches the unprecedented sensitivity of  $10^{-13}$  for  $\mu^+ \rightarrow e^+ \gamma$ . Later we can expect the sensitivity to reach  $10^{-14}$ . On the  $\mu$ - $e$  conversion front, we hope to see  $10^{-16}$  and, in the more distant future,  $10^{-18}$ . These high-sensitivity lower-energy particle physics experiments will reach beyond the 1000-TeV energy scales and thereby will provide highly complementary and competitive probes of new physics, which in turn will help us unravel the puzzles that we hope to encounter through direct discoveries at the LHC. Should new physics not reveal itself at the LHC, these experiments will provide some of the best ways to experimentally probe beyond the standard model; as such, they are a critical component of the overall particle physics scientific program. These are exciting times: We are now working in the regime of LFV sensitivity where we can expect to see a positive signal that can only be interpreted in terms of physics beyond the standard model.

## DISCLOSURE STATEMENT

The authors are not aware of any biases that might be perceived as affecting the objectivity of this review.

## ACKNOWLEDGMENTS

The work of W.J.M. was supported by U.S. Department of Energy grant number DE-AC02-76CH00016. The work of T.M. was supported by a Ministry of Education, Culture, Sports, Science and Technology Grant-in-Aid for Scientific Research on Priority Areas 441. J.M.R. acknowledges support by the Natural Sciences and Engineering Research Council, Canada.

## LITERATURE CITED

1. Yao WM, et al. (Particle Data Group Collab.) *J. Phys. G* 33:1 (2006)
2. Barate R, et al. (LEP Higgs Work. Group Collab.) *Phys. Lett. B* 565:61 (2003)
3. Alcaraz J, et al. (ALEPH, DELPHI, L3, OPAL Collab.) hep-ex/0712.0929 (2007)
4. Glashow S, Iliopoulos J, Maiani L. *Phys. Rev. D* 2:1285 (1970)
5. Abe K, et al. (Belle Collab.) *Phys. Rev. D* 66:071102 (2002)

6. Aubert B, et al. (BaBar Collab.) *Phys. Rev. Lett.* 89:201802 (2002)
7. Hinks E, Pontecorvo B. *Phys. Rev.* 73:257 (1948)
8. Lokanathan S, Steinberger J. *Phys. Rev.* 98:240(A) (1955)
9. Feinberg G. *Phys. Rev.* 110:1482 (1958)
10. Danby G, et al. *Phys. Rev. Lett.* 9:36 (1962)
11. Pontecorvo B. *Sov. Phys. JETP* 37:1236 [trans. JETP 37:1751 (1959)] (1960)
12. Schwarz M. *Phys. Rev. Lett* 4:306 (1960)
13. Pontecorvo B. *Sov. Phys. JETP* 7:172 (1958)
14. Maki Z, Nakagawa M, Sakata S. *Prog. Theor. Phys.* 28:870 (1962)
15. Bertl W, et al. (SINDRUM II Collab.) *Eur. Phys. J. C* 47:337 (2006)
16. Marciano WJ, Sanda AI. *Phys. Rev. Lett.* 38:1512 (1977)
17. Marciano WJ, Sanda AI. *Phys. Lett. B* 67:303 (1977)
18. Kuno Y, Okada Y. *Rev. Mod. Phys.* 73:151 (2001)
19. Czarnecki A, Marciano WJ, Melnikov K. *AIP Conf. Proc.* 435:409 (1998)
20. Kitano R, Koike M, Okada Y. *Phys. Rev. D* 66:096002 (2002)
21. Czarnecki A, Marciano WJ. *Phys. Rev. D* 64:013014 (2001)
22. Stockinger D. *J. Phys. G* 34:R45 (2007)
23. Chacko Z, Kribs GD. *Phys. Rev. D* 64:075015 (2001)
24. Graesser M, Thomas SD. *Phys. Rev. D* 65:075012 (2002)
25. Pifer AE, Bowen T, Kendall KR. *Nucl. Instrum. Methods* 135:39 (1976)
26. Kuno Y, Maki A, Okada Y. *Phys. Rev. D* 55:2517 (1997)
27. Brooks ML, et al. (MEGA Collab.) *Phys. Rev. Lett.* 83:1521 (1999)
28. Ahmed M, et al. (MEGA Collab.) *Phys. Rev. D* 65:112002 (2002)
29. Mori T, et al. (MEG Collab.) *UT-ICEPP* 00-02 (1999)
30. Hisamatsu Y. (MEG Collab.) *Eur. Phys. J. C* 52:477 (2007)
31. Ootani W, et al. (MEG Collab.) *IEEE Trans. Appl. Supercond.* 14:568 (2005)
32. Mihara S, et al. (MEG Collab.) *Cryogenics* 44:223 (2004)
33. Ritt S. (MEG Collab.) *Nucl. Instrum. Methods A* 494:520 (2002)
34. Baldini A, et al. (MEG Collab.) *Nucl. Instrum. Methods A* 545:753 (2005)
35. Mihara S, et al. (MEG Collab.) *Cryogenics* 46:688 (2006)
36. Baldini A, et al. (MEG Collab.) *Nucl. Instrum. Methods A* 565:589 (2006)
37. Bellgardt U, et al. (SINDRUM Collab.) *Nucl. Phys. B* 299:1 (1988)
38. Bertl W, et al. (SINDRUM Collab.) *Nucl. Phys. B* 260:1 (1985)
39. Bachman M, et al. (MECO Collab.) *BNL Proposal E 940* (1997)
40. Dzhilkibaev RM, Lobashev VM. (MELC Collab.) *Sov. J. Nucl. Phys.* 49:384 (1989)
41. Carey RM, et al. (Mu2e Collab.) *Fermilab Letter of Intent.* (2007)
42. Bryman D, et al. (COMET Collab.) *J-PARC Proposal P21.* (2007)
43. Kuno Y, et al. (PRISM Collab.) *J-PARC Letter of Intent.* (2006)
44. Bona M, et al. *SuperB: A High-Luminosity Asymmetric  $e^+e^-$  Super Flavour Factory, Conceptual Design Report.* SLAC-R-709, INFN-AE-07-02, LAL-07-15 (2007)
45. Babu KS, Kolda C. *Phys. Rev. Lett.* 89:241802 (2002)
46. Sher M. *Phys. Rev. D* 66:057301 (2002)
47. Brignole A, Rossi A. *Nucl. Phys. B* 701:3 (2004)
48. Antusch S, Arganda E, Herrero MJ, Teixeira AM. *JHEP* 11:90 (2006)
49. Aubert B, et al. (BaBar Collab.) *Nucl. Instrum. Methods A* 479:1 (2002)
50. Abashian A, et al. (Belle Collab.) *Nucl. Instrum. Methods A* 479:117 (2002)
51. Banerjee S, Pietrzyk B, Roney JM, Was Z. *Phys. Rev. D* 77:054012 (2008)
52. Aubert B, et al. (BaBar Collab.) *Phys. Rev. Lett.* 95:041802 (2005)
53. Hayasaka K, et al. (Belle Collab.) hep-ex/0705.0650 (2007)
54. Aubert B, et al. (BaBar Collab.) *Phys. Rev. Lett.* 96:041801 (2006)
55. Narsky IV. *Nucl. Instrum. Methods A* 450:444 (2000)
56. Cousins RD, Highland VL. *Nucl. Instrum. Methods A* 320:331 (1992)
57. Barlow R. *Comput. Phys. Commun.* 149:97 (2002)

58. Miyazaki Y, et al. (Belle Collab.) hep-ex/0711.2189 (2007)
59. Aubert B, et al. (BaBar Collab.) *Phys. Rev. Lett.* 99:251803 (2007)
60. Miyazaki Y, et al. (Belle Collab.) *Phys. Lett. B* 648:341 (2007)
61. Aubert B, et al. (BaBar Collab.) *Phys. Rev. Lett.* 98:061803 (2007)
62. Miyazaki Y, et al. (Belle Collab.) *Phys. Lett. B* 639:159 (2006)
63. Aubert B, et al. (BaBar Collab.) hep-ex/0711.0980 (2007)
64. Nishio Y, et al. (Belle Collab.) hep-ex/0801.2475 (2007)
65. Aubert B, et al. (BaBar Collab.) *Phys. Rev. Lett.* 95:191801 (2005)
66. Yusa Y, et al. (Belle Collab.) *Phys. Lett. B* 640:138 (2006)
67. Hewett Joanne L, ed. *The Discovery Potential of a Super B Factory. SLAC Workshops.* SLAC-R-709 (2004)
68. Hashimoto ES, et al. *Letter of intent for KEK super B factory*, KEK-REPORT-2004-4 (2004)
69. Raidal M, et al. hep-ph/0801.1826 (2008)
70. Unel NG. hep-ex/0505030 (2005)
71. Pati JC, Salam A. *Phys. Rev. D* 10:275 (1974)
72. Landsberg LG. *Phys. Atom. Nucl.* 68:1190 (2005)
73. Sher A, et al. *Phys. Rev. D* 72:012005 (2005)
74. Ambrose D, et al. (BNL Collab.) *Phys. Rev. Lett.* 81:5734 (1998)
75. Abouzaid E, et al. (KTeV Collab.) hep-ex/0711.3472 (2007)
76. White DB, et al. *Phys. Rev. D* 53:6658 (1996)
77. Aitala EM, et al. (E791 Collab.) *Phys. Lett. B* 462:401 (1999)
78. Aubert B, et al. (BaBar Collab.) *Phys. Rev. Lett.* 93:191801 (2004)
79. Aubert B, et al. (BaBar Collab.) hep-ex/0712.1516 (2007)
80. Bornheim A, et al. (CLEO Collab.) *Phys. Rev. Lett.* 93:241802 (2004)
81. Aubert B, et al. (BaBar Collab.) *Phys. Rev. D* 73:092001 (2006)
82. Aubert B, et al. (BaBar Collab.) *Phys. Rev. Lett.* 99:201801 (2007)
83. Abe F, et al. (CDF Collab.) *Phys. Rev. Lett.* 81:5742 (1998)
84. Bai JZ, et al. (BES Collab.) *Phys. Lett. B* 561:49 (2003)
85. Ablikim M, et al. (BES Collab.) *Phys. Lett. B* 598:172 (2004)
86. Aubert B, et al. (BaBar Collab.) *Phys. Rev. D* 75:031103 (2007)
87. Bernreuther W, et al. In *Proc. Workshop Z Phys. LEP*, ed. G Altarelli, R Kleiss, C Verzegnassi, Vol. 2, p. 34. Zurich: CERN 89-08 (1989)
88. ALEPH, DELPHI, L3, OPAL, SLD Collab.; LEP Electroweak Work. Group; SLD Electroweak Heavy Flavour Group. *Phys. Rep.* 427:257 (2006)
89. Marciano WJ. *Nucl. Phys. Proc. Suppl.* 40:3 (1995)
90. Akers R, et al. (OPAL Collab.) *Z. Phys. C* 67:555 (1995)
91. Abreu P, et al. (DELPHI Collab.) *Z. Phys. C* 73:243 (1997)
92. Bolton RD, et al. *Phys. Rev. Lett.* 53:1415 (1984)